Science of the Total Environment 917 (2024) 170239

Contents lists available at ScienceDirect

Science of the Total Environment

journal homepage: www.elsevier.com/locate/scitotenv

# Coastal adaptation and migration dynamics under future shoreline changes

Lars Tierolf [a,*], Toon Haer [a], Panagiotis Athanasiou [b], Arjen P. Luijendijk [b,c], W.J. Wouter Botzen [a,d], Jeroen C.J.H. Aerts [a,b]

[a] Institute for Environmental Studies, VU University Amsterdam, Amsterdam, the Netherlands
[b] Deltares, Delft, the Netherlands
[c] Faculty of Civil Engineering and Geosciences, Delft University of Technology, Delft, the Netherlands
[d] Utrecht University School of Economics, Utrecht University, Utrecht, the Netherlands

## HIGHLIGHTS

- We model household adaptation and migration behavior in face of coastal erosion and increasing flood risk in France.
- We find without considering coastal adaptation, a worst-case sea level rise could induce the cumulative out-migration of up to 21,700 people residing in the 1/100-year flood zone (3.7 %) by 2080.
- Beach renourishment and household adaptations reduced this projected net outmigration to 13,800 people (2.3 %) under the same scenario.
- Not accounting for coastal erosion could result in underestimations of sea level rise induced migration.
- The modeling framework presented in this paper addresses multiple environmental impacts of sea level rise on coastal communities.

## GRAPHICAL ABSTRACT

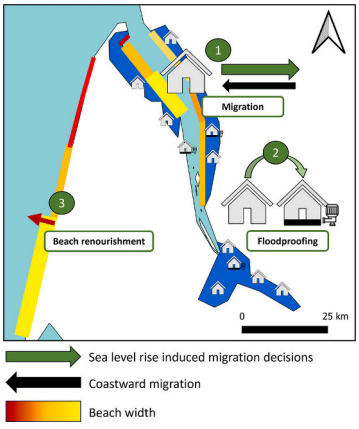


## ARTICLE INFO

Editor: Sergi Sabater

*Keywords:*
Sea level rise
Coastal adaptation
Climate migration
Flood risk
Coastal erosion
Agent-based modeling

## ABSTRACT

In this study, we present a novel modeling framework that provides a stylized representation of coastal adaptation and migration dynamics under sea level rise (SLR). We develop an agent-based model that simulates household and government agents adapting to shoreline change and increasing coastal flood risk. This model is coupled to a gravity-based model of migration to simulate coastward migration. Household characteristics are derived from local census data from 2015, and household decisions are calibrated based on empirical survey data on household adaptation in France. We integrate projections of shoreline retreat and flood inundation levels under two Representative Concentration Pathways (RCPs) and account for socioeconomic development under two Shared Socioeconomic Pathways (SSPs). The model is then applied to simulate coastal adaptation and migration between 2015 and 2080. Our results indicate that without coastal adaptation, SLR could drive the cumulative net outmigration of 13,100 up to as many as 21,700 coastal inhabitants between 2015 and 2080 under SSP2–RCP4.5 and SSP5–RCP8.5, respectively. This amounts to between 3.0 %–3.7 % of the coastal

* Corresponding author.
*E-mail address:* lars.tierolf@vu.nl (L. Tierolf).

https://doi.org/10.1016/j.scitotenv.2024.170239
Received 19 September 2023; Received in revised form 9 January 2024; Accepted 15 January 2024
Available online 24 January 2024

population residing in the 1/100-year flood zone in 2080 under a scenario of SLR. We find that SLR-induced migration is largely dependent on the adaptation strategies pursued by households and governments. Household implementation of floodproofing measures combined with beach renourishment reduces the projected SLR-induced migration by 31 %–36 % when compared to a migration under a scenario of no adaptation. A sensitivity analysis indicates that the effect of beach renourishment on SLR-induced migration largely depends on the level of coastal flood protection offered by sandy beaches. By explicitly modeling household behavior combined with governmental protection strategies under increasing coastal risks, the framework presented in this study allows for a comparison of climate change impacts on coastal communities under different adaptation strategies.

## 1. Introduction

Today, over 100 million people inhabit the coastal 1/100-year floodplain, an area that is flooded on average once every 100 years. This population is projected to increase to 260 million in 2100 (Merkens et al., 2018). Sandy shorelines comprise 31 % of the world's ice-free coastline, providing coastal inhabitants with natural flood protection and amenities (Luijendijk et al., 2018; Temmerman et al., 2013). Twenty-four percent of the world's sandy beaches are currently eroding, with rates exceeding 0.5 m/year (Luijendijk et al., 2018). Sea level rise (SLR) increases relative storm surge heights and subsequent inundation level, in turn increasing the coastal flood risk for exposed populations (Muis et al., 2020). Rises in sea levels further result in shoreline recession as beach profiles adjust to the new prevailing wave conditions (Zhang et al., 2004). The combined effect of increased storm surge height and beach profile adjustment could cause up to 46 % of the world's sandy beaches to retreat by >100 m by 2100 (Vitousek et al., 2017; Vousdoukas et al., 2020; Zhang et al., 2004).

The loss of sandy beaches affects coastal communities through changes in natural flood protection and the loss of coastal amenities (Gopalakrishnan et al., 2011; Landry et al., 2022; McNamara et al., 2015; Nicholls, 1998; Toimil et al., 2023). In some areas, this increasing flood risk may drive people out of the coastal floodplain, a process potentially exacerbated by reduced attractiveness through the loss of sandy beach amenities (Hauer et al., 2020). SLR-induced changes in flood risk and erosion rates could spur the migration of millions of coastal inhabitants before the end of this century (Hinkel et al., 2013; Lincke and Hinkel, 2021). However, households and governments may adapt to these changes in their environments, affecting the migration response of communities exposed to SLR (Reimann et al., 2023).

Households adapt to coastal flood risk by elevating their homes and implementing floodproofing measures, such as placing appliances at a higher elevation, installing floodwater pumps, or using flood-proof building materials (Koerth et al., 2017). Governments adapt by building (or upgrading existing) flood protection infrastructure and by renourishing eroding beaches (Aerts et al., 2018). Lincke and Hinkel (2018) found that structural measures, such as dikes, are economically feasible for protecting 13 % of the global coastline, which accounts for 90 % of the global coastal floodplain population. The Netherlands is a prime example of a country relying on structural measures; most of its population residing in the coastal flood zone is protected against flood events with recurrence intervals of 10,000 years (Scussolini et al., 2016). In Belgium, the coastal flooding of 1973 led to the Sigma project. This project aims to protect the inhabitants of the Schelde estuary against flooding with similar recurrence intervals through the elevation and strengthening of dikes (Marchand et al., 2006). Further implementation and upgrading of structural measures could significantly reduce future coastal flood damages due to SLR on a global scale (Tiggeloven et al., 2020).

In addition to raising dikes and levees, beach renourishment can be applied as an alternative (or complementary) strategy for coastal protection (Bird and Lewis, 2015b; Temmerman et al., 2013). The practice of renourishing eroding beaches is well established in the United States and Europe (Houston., 2022; Pranzini et al., 2015). Beach renourishment involves enhancing the sediment budget with sand or gravel dredged from harbors or designated borrow areas (Bird and Lewis, 2015a). Often, renourishment is accompanied by groins and other hard infrastructure to minimize the rate of sediment loss (Hanson et al., 2002). Adaptation to SLR through beach renourishment and floodproofing on the property level could reduce the (future) migration of people exposed to SLR. Beach renourishment maintains the coastal amenity value and enhances coastal flood protection, while property floodproofing reduces a household's vulnerability to flooding (Aerts et al., 2018; Hauer et al., 2020).

Modeling studies on the impacts of SLR on coastal populations tend to focus only on forced displacement due to permanent inundation (Hauer, 2017), increased frequency of coastal flooding (Lincke and Hinkel, 2021), or coastal erosion (Hinkel et al., 2013) but do not consider their combined effect on adaptation responses. The impacts of SLR on coastal communities are affected by adaptations to increasing flood risk, such as floodproofing and migration, which are in turn influenced by governmental protection schemes and individual characteristics (Hauer et al., 2020). A research need exists for modeling such interactions from the "bottom up," while considering the household characteristics from which the adaptation response emerges (Horton et al., 2021).

In this study, we develop a new erosion module within DYNAMO-M, a coupled agent-based gravity model that simulates a household's migration and adaptation decisions in the coastal floodplain while considering sustained coastward migration from inland areas (de Ruig et al., 2022; Haer et al., 2019; Tierolf et al., 2023). We integrate socioeconomic scenarios, shoreline change projections, and beach renourishment decisions in this model of coastal adaptation dynamics. The novelty of the methodology presented in this study lies in incorporating global projections of shoreline retreat with governmental protection schemes through beach renourishment in a model of household adaptation and migration behavior. We apply DYNAMO-M, augmented with coastal erosion, to simulate coastal adaptation behavior in the 1/100-year flood zone from 2015 to 2080 in France. By explicitly modeling the effects of SLR-enhanced coastal erosion on household adaptation and migration decisions, we aim to develop a model framework that allows for a comparison of SLR impacts on coastal communities under different adaptation strategies.

## 2. Case study area

The French coastline has seen extensive development over the past 60 years (Pranzini et al., 2015). The population in the 1/100-year flood zone is projected to further increase from 1.6 million in 2000 to 2.33 million in 2060 (Neumann et al., 2015). In the French Riviera, many coastal resorts and yachting harbors were constructed between 1965 and 1980, often at the expense of natural beaches (Anthony, 1997). Areas that were previously sparsely populated on the Atlantic coast due to coastal erosion experienced a population increase exceeding 60 % between 1960 and 2000 (Lins-de-Barros et al., 2019). Development mostly occurred on low-lying and often reclaimed land, protected only by narrow stretches of coastal dunes. The erosion of these dune systems could result in extensive storm-induced marine flooding before 2050 (Crapoulet et al., 2016; Maspataud et al., 2013).

The government of France has instituted several spatial planning laws to manage coastal risks. The *Conservatoire du Littoral et des Rivages*

*Lacustres* (1975) allows the government to acquire coastal areas to manage land use and restore and protect coastal wetlands (Pranzini et al., 2015). The coastal law (*loi Littoral*) of 1986 prohibits new urban development within 100 m from the upper limit of the shoreline. Since 1995, French municipalities must adhere to their Coastal Risk Prevention Plans (PPRLs) in pre-defined coastal flooding and erosion hazard zones, which outline measures that reduce risk, such as implementing flood protection infrastructure and zoning laws (Audère and Robin, 2021; Deboudt, 2010). This erosion hazard zone is determined by extrapolating historic shoreline retreat 100 years into the future and adding to this the maximum shoreline retreat in an extreme storm event (*DDTM*, 2015). However, most PPRLs do not account for the impacts of SLR on future coastal risks, and many municipalities still allow for commercial and residential development within hazardous zones (Chadenas et al., 2014; Robert and Schleyer-Lindenmann, 2021). In many areas, the costs of defending these properties already exceed their value or the financial means of local authorities, forcing the national government to resort to expropriation (Meur-Férec et al., 2008).

Incentives through the mandatory insurance scheme *Catastrophes Naturelles* play only a minor role in household decisions to implement floodproofing measures, and government subsidies are rarely applied to finance them (Barraqué and Moatty, 2020; Poussin et al., 2013). Individual households thus make decisions to finance and implement floodproofing measures or to relocate out of the coastal floodplain on their own. Poussin et al. (2013) found that although many households residing in flood-prone areas in France had implemented some form of wet floodproofing measures (e.g., 78 % of respondents had positioned electronic appliances above likely flood levels), the implementation rate of structural dry floodproofing measures was low (e.g., 21 % had strengthened their property foundations against water pressures). The lack of structural flood adaptation in hazard zones by households could thus be explained by their low flood risk perception, accompanied by budget constraints due to a lack of government subsidies (Durand et al., 2018; Koerth et al., 2017; Poussin et al., 2014).

To protect the population and assets in the coastal zone against marine flooding, coastal managers in France typically rely on hard infrastructure, such as sea walls and dikes (Hanson et al., 2002). Beach renourishment is only sparsely applied; between 1962 and 2000, an estimated volume of 12 million $m^3$ of sand was applied to beach renourishment projects in the whole of France, with an average annual fill rate of 0.7 million $m^3$ of sand per year (Hanson et al., 2002). This is much lower than fill rates in the United Kingdom (4 million $m^3$/year) or Spain (10 million $m^3$/year; Hanson et al., 2002). However, the number of nourishment projects to preserve and restore sandy beaches for tourism and flood protection is increasing (Pranzini et al., 2015). For example, in 2014, a total volume of 1.5 million $m^3$ of sand was applied to widen beaches and increase protection against coastal flooding in several residential districts in Dunkirk (Spodar et al., 2018).

Since the elevation of existing homes is not considered a cost-effective strategy (Aerts et al., 2014; Poussin et al., 2015) and many households in France have already implemented some form of wet floodproofing measures (Poussin et al., 2013), we focused on modeling the implementation of dry floodproofing measures by households. We modeled household decisions to migrate or implement dry floodproofing measures using an agent-based model (ABM). ABMs allow researchers to model interpersonal differences in risk perceptions and their influence on adaptation and migration decisions (Bell et al., 2021; Haer et al., 2019; Klabunde and Willekens, 2016). We captured beach renourishment by simulating a government that could offset shoreline retreat by renourishing sandy beaches. Beach renourishment affected household decision-making by maintaining the attractiveness of residing close to a sandy beach and by reducing coastal flood risk through preserving the coastal protection offered by sandy beaches. We assumed that dikes and levees protecting homes that are not directly adjacent to sandy beaches are continuously raised to match the projected SLR. The model thereby aims to provide a stylized representation of household behavior and beach renourishment in the face of SLR.

## 3. Methodology

### 3.1. Model framework

In this study, we develop a new erosion module within the coupled DYNAMO-M agent-based gravity model (de Ruig et al., 2022; Haer et al., 2019; Tierolf et al., 2023). DYNAMO-M consists of an ABM that simulates household adaptation and migration behavior in the coastal floodplain, coupled to a gravity-based migration model that simulates migration toward the coastal floodplain and between inland regions (Fig. 1). We have simulated household adaptation and migration decisions in response to increasing coastal flood risk using an integrated flood risk model at yearly timesteps between 2015 and 2080 (Huizinga et al., 2017).

The study area of France was first divided into departments (NUTS-3 administrative units), with inland departments represented by inland nodes. Each coastal department was split into a coastal zone and an inland zone using the 1/100-year coastal flood map of 2080 under RCP8.5 (Ward et al., 2020). The inland zone of the department is represented by an inland node, whereas the coastal zone is represented by a coastal node. Both inland and coastal nodes contain information on income and population size, but only households residing in coastal nodes are made spatially explicit in 1 km-by-1 km grid cells.

Households in the coastal nodes experience increasing water levels as a direct effect of SLR and the loss of natural coastal flood protection and coastal amenity value due to increasing beach erosion rates (see *model inputs* below). Household agents can decide to adapt to these changes by implementing dry floodproofing measures, or they may migrate out of the current floodplain toward other coastal or inland areas (see *household decisions* below). We further simulated a government agent acting on all coastal nodes, which can offset coastal erosion through beach renourishment (see *government decisions* below). Households in the inland nodes were simulated as an aggregated population to reduce computational demand. The ABM simulated adaptation behavior in each coastal node (household floodproofing and migration, and beach renourishment), while a gravity-based migration model simulated internal migration flows toward the coastal nodes and between the inland nodes.

Migration flows in the model were simulated in three different ways. *Migration flows from coastal nodes toward all other nodes* were simulated using the ABM and discounted subjective utility theory (DEU; see *household decisions* below). Households were assumed to migrate when the utility of migration to a node had exceeded the utility of remaining in the coastal node (with and without implementing floodproofing). *Migration toward coastal and between inland nodes* was simulated using a calibrated gravity-based model of migration (see *gravity model* below). *The distribution of coastal in-migration from all nodes* was simulated at the end of each timestep by the ABM. After all migration flows had been simulated, the households moving into coastal nodes from both inland and other coastal nodes were spatially distributed in 1 km-by-1 km grid cells in the 1/100-year floodplain based on flood risk (mediated by the perception of the household) and coastal amenity value (see *coastal in-migration* below).

Population growth, economic development, and SLR were simulated under Representative Concentration Pathways (RCP) paired with Shared Socioeconomic Pathway (SSP) scenarios (van Vuuren et al., 2014). A model description following the overview, design concepts and details plus decisions (ODD+D) protocol (Müller et al., 2013) is provided in the supplementary information.

### 3.2. Model inputs

*Annual inundation levels*: Coastal inundation maps for current and future climate conditions under RCP4.5 and RCP8.5 were retrieved from

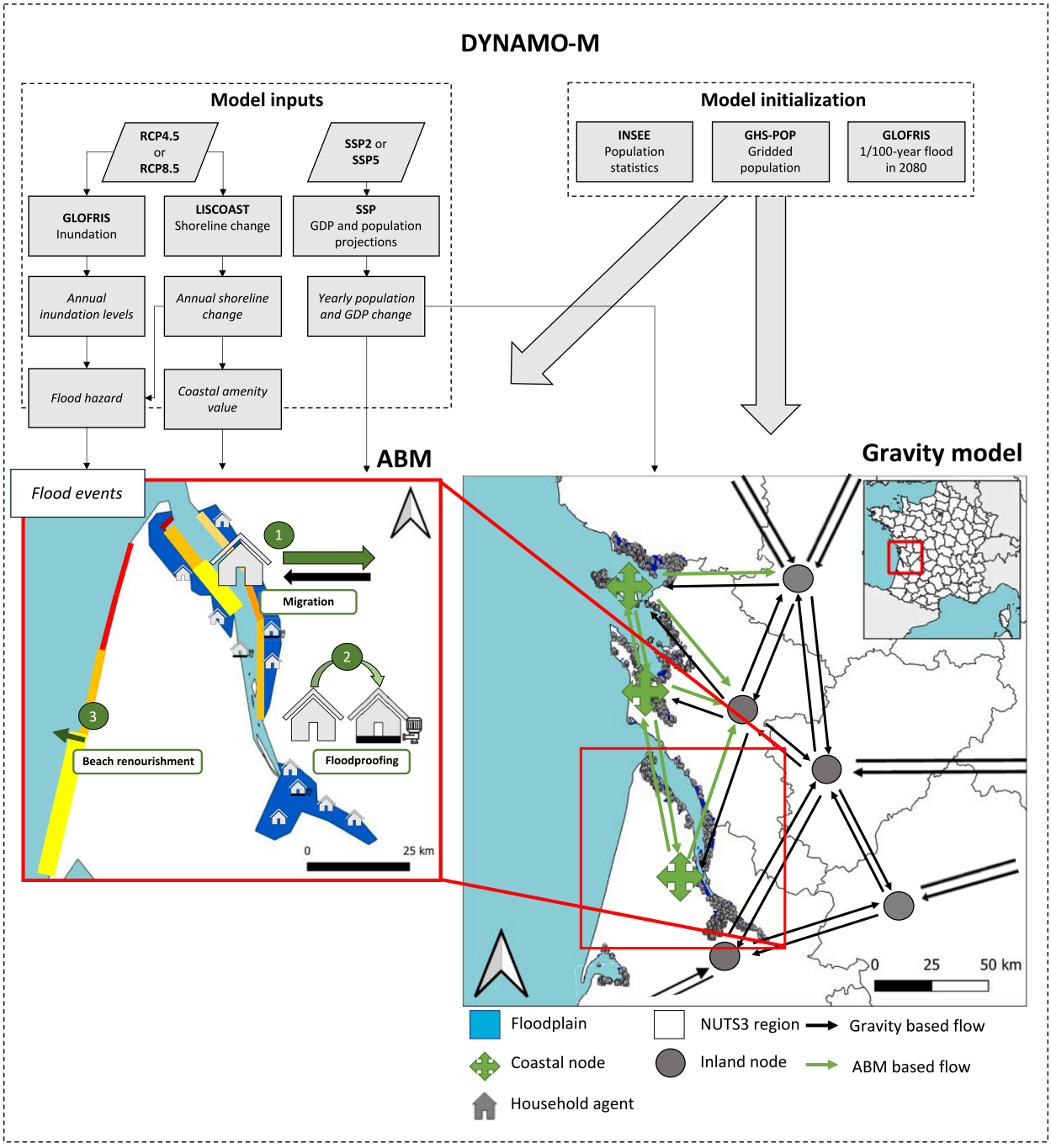


**Fig. 1.** Schematic representation of the DYNAMO-M model framework. An ABM simulates household migration and adaptation decisions considering flood risk and shoreline change under coupled RCP–SSP scenarios (see *model input*). DYNAMO-M is initialized using population statistics on income and wealth, a gridded population map, and a map delineating the 1/100-year floodplain in 2080 under RCP8.5 (*see model initialization*). In each coastal node (green symbols) representing the coastal flood zone of a department (NUTS3 regions), the ABM simulates 1) household migration to other coastal and inland nodes, 2) floodproofing decisions under SLR and socioeconomic development, and 3) government adaptation by renourishing eroding beaches. Each year, floods may occur, randomly drawn from a distribution with annual inundations associated with return periods of up to 1 in 1000 years. This ABM is coupled to a gravity model that simulates migration between inland nodes and toward coastal nodes. Note that, for clarity, only a part of France is shown, and not all linking arrows are drawn.

the GLOFRIS modeling framework (van Vuuren et al., 2011; Ward et al., 2020). The flood maps contain inundation levels associated with flood events with return periods of 2, 5, 10, 20, 50, 100, 200, 500 and 1000 years in a spatial resolution of 1 km by 1 km. Inundation maps for 2030, 2050, and 2080 under RCP4.5 and RCP8.5 were constructed by combining gridded projections of SLR with estimations of land subsidence (Jevrejeva et al., 2014; Ward et al., 2020). To derive annual inundation levels under RCP4.5 and RCP8.5, we interpolated between historical and projected (2030, 2050, and 2080) flood levels (de Ruig et al., 2023; Tierolf et al., 2023). Based on the climate scenario specified in the model run, the inundation levels for each household were sampled for all return periods for its current location in the floodplain.

*Annual shoreline change*: We used global shoreline change trends and projections developed under the LISCOAST project to simulate shoreline change for sandy coastal segments under RCP4.5 and RCP8.5 (Luijendijk et al., 2018; Vousdoukas et al., 2020). The dataset contains probabilistic

shoreline change projections for 2050 and 2100 relative to 2010 under RCP4.5 and RCP8.5. These projections were generated by combining observed shoreline trends with morphological shoreline adjustment driven by SLR using the calibrated Bruun rule (Bruun, 1962). Although the generic applicability of the Bruun rule to capture shoreline change under SLR has caused considerable debate (Cooper et al., 2020; Pilkey et al., 2000; Stive, 2004), this shoreline change model is consistent with most long-term morphodynamical beach models (Dean and Houston, 2016; Passeri et al., 2014; Zhang et al., 2004) and is applicable on the national scale (Athanasiou et al., 2020; Ranasinghe, 2020).

The LISCOAST dataset consists of coastal segments 500 m in length, which have been aggregated here in 1-km segments to match the inundation level resolution. Following Vousdoukas et al. (2020), we assumed an initial beach width of 100 m at the beginning of each model run (2015). We interpolated annual shoreline changes by fitting a polynomial of 2 degrees on the median of projected shoreline retreat in 2050 and 2100.

*Yearly population and economic development*: Population development and economic growth under SSPs were coupled to the RCPs using a scenario matrix (van Vuuren et al., 2014). The SSP2 (*middle of the road*) scenario was coupled to RCP4.5, while SSP5 (*fossil-fueled development*) was coupled to RCP8.5. Natural population change under the SSPs was distributed over departments by adjusting their current fertility rates (Tierolf et al., 2023). The change in gross domestic product (GDP) projected in the SSPs was used to adjust household wealth, income, property value, and the cost of adaptation and migration. The applied population and GDP projections are provided in Supplementary Fig. S1.

*Flood events*: We simulated flood events via random draws for each department and the exceedance probability of each flood event (e.g., a 1/10-year flood has a 10 % percent chance of occurring each timestep, a 1/200-year flood a 0.5 % chance, etc.), after which all households residing in the floodplain of the flood event were expected to experience flooding and update their risk perceptions (see *household decisions*). We only accounted for flooding with return periods that exceed the current flood protection standard (FPS) and assumed a coastal flood protection standard of 1/10-years for all coastal areas in France (Tourment et al., 2018).

Coastal erosion can affect natural flood protection through the erosion of dunes and decreases in dune crest height, resulting in more frequent dune overtopping (Benavente et al., 2006). Changes in beach profile further alter wave setup, potentially increasing inundation levels (Toimil et al., 2023). Studies aimed at quantifying the interaction and coupling of coastal erosion and flooding often assess these interactions on the scale of individual beaches (Toimil et al., 2023), up to the scale of bays or inlets (Benavente et al., 2006; Passeri et al., 2016). Studies at larger scales are often limited by the unavailability of high-quality morphological data and computational power (Ranasinghe, 2020). However, the effect of coastal erosion on coastal inundation levels and extent may be greater than the effect of SLR alone and should thus be accounted for in studies of coastal responses to SLR (Toimil et al., 2023). To account for the effect of coastal erosion on flood protection for beachfront properties, we assumed that the FPS for households within 1 km of an eroding sandy beach segment is reduced to 1 in 5 years once shoreline retreat exceeds 100 m.

### 3.3. Model initialization

We generated an agent population in each 1 km-by-1 km raster cell of each coastal node by sampling individuals from a gridded population map of 2015 overlayed with the 1/100-year coastal floodplain of 2080 under RCP8.5 (Schiavina et al., 2019; Ward et al., 2020). Individuals were grouped into household agents of an average household size of 3.5 people using a random uniform distribution ranging from 1 to 6. Households were assigned positions in a subnational lognormal income distribution reflecting various professions. This position was used to assign each household's wealth and disposable income using subnational statistics (INSEE, 2017). In each timestep, households assessed their current flood damages by sampling from the inundation maps of all return periods using household-specific depth-damage curves (Huizinga et al., 2017). To create an agent population in which some of the households had already implemented adaptation measures, all model runs were initiated with a calibrated spin-up period of 15 years, during which we simulated household migration and adaptation decisions. The parameters applied during this spin-up period were calibrated based on the observed implementation rate of dry floodproofing measures in France (see *model calibration* and *household decisions*). Since datasets on current beach width were not available, we assumed that beaches all had an initial width 100 m in 2015 and simulated beach renourishment during the spin-up period.

### 3.4. Household decisions

Households residing in the coastal 1/100-year flood zone were assumed to make decisions based on subjective time-discounted expected utility theory (DEU; Fishburn, 1981), a commonly applied decision theory in ABMs of household adaptation and migration (Bell et al., 2021; De Koning and Filatova, 2020; de Ruig et al., 2022; Haer et al., 2019). DEU allows for a direct weighing of a household's adaptation strategies while accounting for subjective risk perceptions and risk preference over time, considering experiences with flooding (Di Baldassarre et al., 2013; Haer et al., 2017). Individual agents aim to maximize the utility outcome of each decision, considering the bounded rationality of risk perceptions (see *bounded rationality* below). At each timestep, representing 1 year, each household was assumed to evaluate the following strategies:

1) Doing nothing (Eq. (1));
2) Implementing dry floodproofing measures (Eq. (2)); and
3) Migrating to department *y* (Eq. (3))

$$DEU_1 = \int_{p_i}^{p_I} \beta_t * p_i * U\left(\sum_{t=0}^{T} \frac{W_x + A_x + Inc_x - D_{x,i}}{(1+r)^t}\right) dp \quad (1)$$

$$DEU_2 = \int_{p_i}^{p_I} \beta_t * p_i * U\left(\sum_{t=0}^{T} \frac{W_x + A_x + Inc_x - D_{x,i}^{adapt} - C_t^{adapt}}{(1+r)^t}\right) dp \quad (2)$$

$$DEU_3 = U\left(\sum_{t=0}^{T} \frac{W + A + Inc - C_{y,t}^{migration}}{(1+r)^t}\right) \quad (3)$$

In each timestep in the model, each household was assumed to execute the strategy within its budget constraint that yielded the highest subjective time-discounted utility (see *budget constraint* below). Utility was calculated for each event $i$ that had a probability $p_i$ of occurring; *DEU* was calculated as the approximated integral over all events $I$ (de Ruig et al., 2022; Haer et al., 2019; Tierolf et al., 2023), which represents floods with return periods of 1 up to 1000 years (see *model inputs* above), and the event of no flood occurring.

*Risk aversion and time discounting*: We applied a general utility function following constant relative risk aversion (Bombardini and Trebbi, 2012). The model was run with slightly risk-averse households, in which case $U(x) = \mathrm{Ln}(x)$. We applied a time discounting factor ($r$) of 3.2 % specific to France over a decision horizon ($T$) of 15 years, set to reflect the average time a homeowner spends in their home (Evans and Sezer, 2005).

*Calculating utility*: The *DEU* of each strategy is a function of current risk perception ($\beta_t$), current household wealth ($W_x$), current coastal amenity value ($A_x$), current household income ($Inc_x$), the current expected damages without ($D_{x,i}$) and with adaptation ($D_{x,i}^{adapt}$) under each event $I$, and annualized adaptation costs ($C_t^{adapt}$). Although we updated household wealth, amenity value, income, and damages with SLR and economic change in each model timestep in accordance with the

SSP–RCP combination applied in the model run, we assumed households to not have any future expectations of these values within the decision horizon *T*. We also assumed that households could only invest a fixed percentage of their disposable income in floodproofing measures and would only consider floodproofing measures if the investment costs fell within this budget constraint (see *cost of dry floodproofing* and *budget constraint* below). In calculating the *DEU* of migration, additional factors included expected wealth, coastal amenity value, and income in location *y* ($W_y$, $A_y$, $I_y$) and the cost of migration ($C^{migration}$; see *migration decisions* below). Household's current income ($I_x$) were sampled based on their positions in a subnational lognormal income distribution (INSEE, 2017), while wealth ($W_x$) was calculated using ratios of wealth to disposable income (Eurostat, 2020).

*Bounded rationality*: People generally exhibit bounded rational behavior and base their behavioral choices on the limited information available to them (Simon, 1955). For example, perceived flood probabilities differ from objective flood probabilities based on flood experience (Kunreuther, 1996). To capture underestimations of flood risk in the absence of flooding and overestimations of risk when households have just experienced a flood, we modeled a dynamic risk perception ($\beta_t$) that converted the objective flood probabilities to perceived (subjective) probabilities (Haer et al., 2017). We defined $\beta_t$ as a function of the number of years after the most recent flood event (Eq. 4). Risk perception was expected to peak immediately after the flood event, leading to an overestimation of the flooding probability ($\beta_t > 1$). Over time, this perception was expected to decrease, resulting in an underestimation of flooding probability ($\beta_t < 1$). The maximum overestimation of flooding probability *c* was calibrated by Tierolf et al. (2023) using survey data on the uptake of floodproofing measures in France (Poussin et al., 2013; see *model calibration* below).

$$\beta_t = c^{*}1.6^{-d^{*}t} + 0.01 \tag{4}$$

*Flood damages*: To determine flood damages as a function of inundation level, a maximum damage value estimated for France was used together with depth damage curves for residential structures in Europe; both were obtained from Huizinga et al. (2017). Dry floodproofing measures, which prevent water from entering the structure, were captured by altering the depth damage curves so that damage at water levels below 1 m was reduced by 85 %. Inundation above 1 m could overtop the dry floodproofing, resulting in full damage.

*Cost of dry floodproofing*: We assumed that households would obtain personal loans to finance dry floodproofing measures. Based on Hudson (2020), we applied an average adaptation cost of €10,800 per building ($C_0^{building}$), which includes the installing pumps and water barriers. Per-building costs were annualized ($C_t^{adapt}$) using a fixed interest rate (*r*) and loan duration (*n*; Eq. 5), in which households were assumed to pay for dry floodproofing measures only for the remainder of loan duration *n*.

$$C_t^{adapt} = C_0^{building} * \frac{r^{*}(1+r)^{n}}{(1+r)^{n}-1} \tag{5}$$

*Budget constraint*: We followed an expenditure cap definition of affordability and assumed that households could invest a fixed percentage of their disposable income in dry floodproofing measures (Hudson, 2018). If the annual loan cost exceeded this expenditure cap, the household could not invest in dry floodproofing measures. The expenditure cap, interest rate (*r*), and loan duration (*n*) were calibrated by Tierolf et al. (2023) based on the observed implementation rate of dry floodproofing measures in France; see *model calibration* below.

*Migration decisions* (Eq. 3): For each household in each coastal node *x*, the expected utility of migration to each other coastal and inland node *y* was calculated based the expected income and wealth in *y* ($I_y$, $W_y$), amenity value in *y* ($A_y$), and the cost of migration to *y* ($C_y$; Eq. 3). Households were assumed to derive their expected income and wealth from the income and wealth distribution within each destination node based on their current positions in the income distribution. The expected amenity value in each node *y* ($W_y$) was calculated based on the average coastal amenity value experienced by households sharing the same position in the income distribution. Migration cost to node *y* ($C_y$) was a function of geographical distance and fixed migration costs, which captured the psychological costs associated with leaving friends and relatives (Sjaastad, 1962). Based on estimates of fixed migration costs by Kennan and Walker (2011), we set the fixed cost of migration at €250,000, which over distance (*dist*) increased to a maximum migration cost of €500,000 (Eq. (6)).

$$C_y^{migration} = \frac{2^{*}C^{fixed}}{1 + e^{-0.05^{*}dist_{xy}}} \tag{6}$$

*Coastal and beach amenity value*: The amenity value associated with residing near the coast was modeled as a function of distance to the coast and beach width; both functions were parameterized based on hedonic pricing studies, which are based on the concept that property values capitalize on amenity values. The approach has been applied to assign monetary values to a wide variety of amenities, such as urban green space (Czembrowski and Kronenberg, 2016) and unobstructed sea views (Muriel et al., 2008). We assumed that households residing within 10 km of the coastline would receive premiums of up to 60 % of their wealth depending on proximity to the coast (Conroy and Milosch, 2011; Muriel et al., 2008). The value of sandy beaches is capitalized in property prices located close to the shoreline, but this effect decreases for properties located further away from the shoreline (Gopalakrishnan et al., 2011; Landry et al., 2022). Landry et al. (2022) found a marginal willingness to pay ranging from $1769–$$4773 per additional foot (~0.3 m) of beach width for property located closer than 500 ft (~150 m) to the shoreline, which decreased to $285–$1606 when located 2500 ft (~762 m) from the ocean front. Gopalakrishnan et al. (2011) found one additional foot of beach width to result in price premiums of $1440 (0.18 %) and $8800 (1.10 %) for an average oceanfront property value of $800,000 in North Carolina (US).

Based on these studies and to capture the effect of coastal erosion on beach value, households residing in a 1 km-by-1 km grid cell adjacent to a sandy beach received an additional amenity premium as a function of current beach width. Based on the abovementioned hedonic pricing studies, we set this premium at 0.60 % of household wealth per additional meter of beach width. We assumed that beach widths exceeding 30 m would not yield additional amenity value, maximizing beach amenity value at a premium of 17 % of agent wealth.

*Coastal in-migration*: At the beginning of each timestep, migration flows from coastal nodes, generated by the ABM, and from inland nodes, generated by the gravity model, were added to the receiving department. Households migrating toward inland nodes were not required to be spatially explicit and were added to the aggregated population. Households moving toward coastal nodes were made spatially explicit in the 1/100-year floodplain based on the maximization of subjective expected utility (*SEU*, Eq. 7). For each household (*i*) 20 random cells within the coastal floodplain were selected, and each cell (*j*) was assessed for its current coastal amenity value ($A_{j,t}$) and coastal flood risk ($EAD_{j,t}$) mediated by the household's current risk perception ($\beta_t$). The household was then allocated to the cell with the highest expected utility (*SEU*).

### 3.5. Government decisions

We modeled two government adaptation strategies: 1) *renourishment*, in which all erosion on sandy beaches in the 1/100-year coastal floodplain was offset by renourishment; and 2) *none*, in which governments did not renourish beaches. Under Strategy 1, we assumed that the government would maintain an FPS protecting against flooding with 10 year recurrence intervals by heightening dikes and renourishing beaches. Under Strategy 2, we assumed that dikes would be heightened to maintain an FPS of 1/10 years into the future but that the flood

protection offered by beaches could be lost due to erosion.

We considered a total of 629 km of sandy shoreline located in the coastal floodplain for renourishment, of which 346 km are currently retreating under ambient shoreline change (Luijendijk et al., 2018). To calculate the volume of sand required to offset erosion in each model timestep, we followed Houston (2017) and Dean and Houston (2016) and calculated the volume of sand required for each year:

$$\Delta A_t = -L\Delta S_t\left(\frac{W_*}{h_* + B}\right) \tag{8}$$

where $A_t$ represents the area of shoreline loss at time $t$ from a SLR until $t$ ($\Delta S$), $L$ represents the length of the beach, $W_*$ represents the width of the active beach profile, $h_*$ represents closure depth, and $B$ represents berm height (see Fig. 2 for a visual representation). Since we used shoreline change estimations from Vousdoukas et al. (2020), we substituted the annual shoreline recession calculated by $\Delta S\left(\frac{W_*}{h_* + B}\right)$ with estimated shoreline retreat until t ($\Delta X_t$), resulting in Eq. (9):

$$A_t = -L\Delta \mathrm{X_t} \tag{9}$$

The shoreline area produced by beach renourishment ($A_N$) of volume $\Delta V_N$ is given by Eq. (10):

$$A_N = \frac{\Delta V_N}{h_* + B} \tag{10}$$

Completely offsetting the eroded area $\Delta A_{SL}$ with renourishment and solving for $\Delta V_N$ results in Eq. (11):

$$\Delta V_{t,N} = (h_* + B)^*\Delta \mathrm{A_t} \tag{11}$$

We used a global dataset indicating depth of closure ($h_*$) for each coastal segment (Athanasiou et al., 2019), which was also used to provide projections of SLR-induced erosion (Vousdoukas et al., 2020). In the absence of a reliable estimation of berm heigh $B$, we followed Vousdoukas et al. (2020) and used the mean sea level contour as the landward active profile boundary.

To calculate the projected renourishment cost, we multiplied the required sand volume by an estimated sand cost per $m^3$. The cost of beach renourishment in the European Union ranges between €4.6–€10/$m^3$ (Aerts, 2018). We provide results for €7 per $m^3$ and scale this cost annually based on economic growth projected under the SSP.

### 3.6. Gravity model

Migration flows toward coastal nodes and between inland nodes were simulated using a gravity-based model of migration (Anderson, 2011; Ramos, 2016) assuming a migration flow between locations to be dependent on their population sizes, and that this flow would decrease with increasing distance between the locations (Poot et al., 2016; Ravenstein, 1885). The traditional gravity model of population (*Pop*) and distance (*Dist*) was augmented with income (*Inc*) and a coastal dummy variable (*Coastal*) to also capture the effect of coastal amenities and income differentials on migration flows (Eq. (12); Tierolf et al., 2023). The coefficients $\beta_{0-7}$ were calibrated by fitting the model to observed internal migration flows using ordinary least-squares regressions; see *model calibration* below.

$$\begin{aligned}\mathrm{Ln}(Flow_{ij}) =& \beta_0 + \beta_1{}^*ln(Pop_{t,i}) + \beta_2{}^*ln(Pop_{t,j}) \\ &+ \beta_3{}^*ln(Inc_i) + \beta_4{}^*ln(Inc_j) + \beta_5{}^*Coastal_i \\ &+ \beta_6{}^*Coastal_j + \beta_7{}^*ln(Distance_{ij})\end{aligned} \tag{12}$$

### 3.7. Adaptation settings and model runs

We modeled coastal migration and adaptation under the combinations SSP2-RCP4.5 and SSP5-RCP8.5. The amount of SLR-induced migration under each SSP-RCP combination was inferred by comparing the modeled population development in the coastal floodplain under SLR with the population development under a baseline scenario of no SLR. We compared SLR-induced net-out migration under three different coastal adaptation strategies: 1) *NoAdaptation*, 2) *HouseholdAdaptation*, and 3) *FullAdaptation* (see Table 1). Coastward migration, dynamic risk perceptions, population growth, and economic development are simulated under all strategies. We assumed that structural flood protection measures would be raised in accordance with SLR. Households experienced changes in beach amenity and coastal flood risk under all simulated adaptation strategies.

Since the model contains several random processes, such as random flood events and the spatial allocation of households in the coastal floodplain, multiple repetitive runs were created for each behavioral setting under both SSP and RCP combinations. To derive the optimal number of repetitions while considering computational demand, we tested for the convergence of the means and standard deviations of simulated population development, flood risk, and adaptation uptake under SSP5–RCP8.5 in 2080 (Fig. 3). Following de Ruig et al. (2023), we randomly sampled the means and standard deviations of these three variables 100 times using sets of 5–50 repetitions for the three adaptation scenarios assessed in the study (*NoAdaptation*, *HouseholdAdaptation* and *FullAdaptation*). As shown in Fig. 3, the mean of the model outcome remained relatively stable for each set of repetitions assessed. The standard deviations increased from five to approximately 40 repetitions, which can be explained by low-probability flood events not always being captured when considering fewer repetitive runs. The increase in standard deviation flattened around 40–50 repetitions, indicating that 50 repetitions were sufficient to capture the range of model outcomes simulated under the current model settings.

### 3.8. Model calibration

For a description of the calibration procedures of the depth-damage

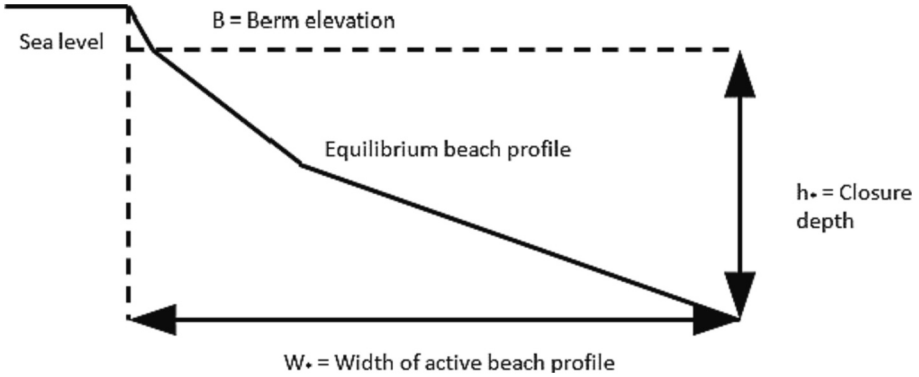


**Fig. 2.** Definitions of $h_*$, B, and $W_*$. Adapted from Houston (2017).

**Table 1**
Simulated adaptation strategies.

| Model setting | Household migration | Household adaptation (dry floodproofing) | Government adaptation (renourishment) |
|---|---|---|---|
| *NoAdaptation* | X | | |
| *HouseholdAdaptation* | X | X | |
| *FullAdaptation* | X | X | X |

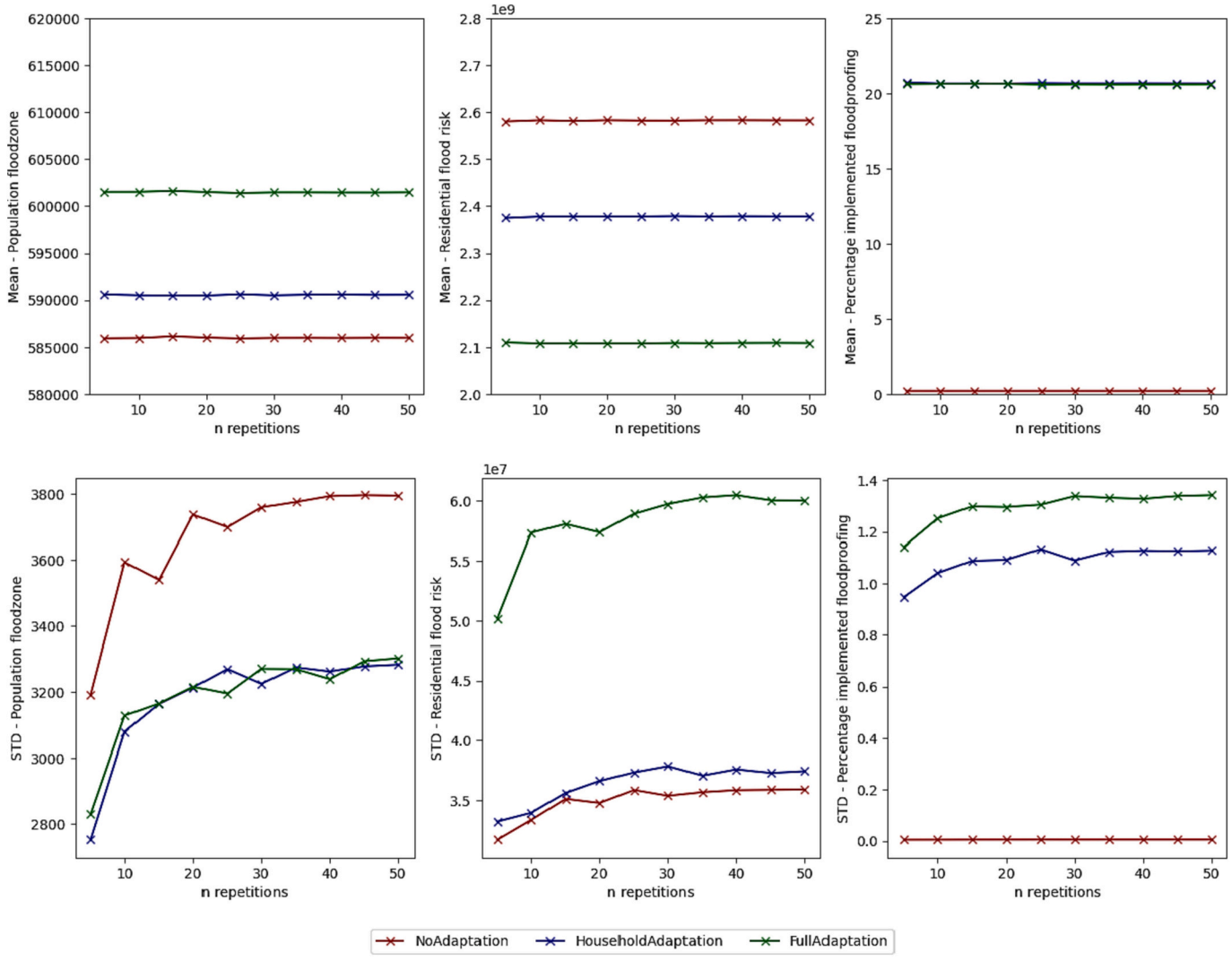


**Fig. 3.** Convergence of mean and standard deviation of model results for 2080 under SSP2-RCP4.5 considering an increasing amount of repetitive model runs. We show the mean of model outcome in the top row. The standard deviation (STD) of model outcomes is presented in the bottom row.

functions and inundation maps applied in the model, we refer to the works of Huizinga et al. (2017) and Ward et al. (2020). Here, we provide a description of the shoreline change projections, household decisions, and gravity model in more detail.

*Shoreline change projections*: The global shoreline projections of Vousdoukas et al. (2020) focus on three components of shoreline change dynamics:

1) Ambient shoreline change dynamics;
2) Morphological adjustment to SLR; and
3) Episodic erosion during extreme storm events.

*Ambient shoreline change dynamics* for coastal segments with an alongshore spacing of 250 m were calibrated on satellite imagery by Luijendijk et al. (2018) and Mentaschi et al. (2018). *Morphological adjustment to SLR* was modeled using the Bruun rule (Bruun, 1962). The underlying concept of this approach is that the beach morphology tends to adjust to a new prevailing wave climate under SLR. Shoreline retreat ($R$) was calculated as a function of the nearshore active beach slope ($\beta$) and the increase in mean sea level ($SLR$; Eq. (13)). Vousdoukas et al. (2020) calibrated the Bruun rule using a global dataset of nearshore active beach slopes (Athanasiou et al., 2019). Probabilistic SLR projections under RCPs were derived from Jackson and Jevrejeva (2016). *Episodic erosion during extreme storm events* was estimated using the KD93 convolution erosion model of Kriebel and Dean (1993). Storm retreat was simulated in a probabilistic manner using projections of storm surge

height and wave action under climate change scenarios (Muis et al., 2016; Vousdoukas et al., 2018). A detailed description of the procedure and links to the datasets can be found in Luijendijk et al. (2018), Mentaschi et al. (2018), and Vousdoukas et al. (2020).

$$R = \frac{1}{tan(\beta)} * SLR \quad (13)$$

*Household decisions*: The household decision rules of the ABM were calibrated by Tierolf et al. (2023) using survey data obtained by Poussin et al. (2013). Risk perception, expenditure caps, and loan interest rates were set so that the modeled implementation rate of floodproofing measures matched the implementation rate observed in the survey at the start of the model. Consistent with the Federal Emergency Management Agency (FEMA) definition of dry floodproofing measures (FEMA, 2021), households were considered to have implemented dry floodproofing measures if they had completed any of the following:

1) Strengthened their foundations against pressures due to floodwater;
2) Implemented water-resistant doors and walls on the ground floor;
3) Installed anti-backflow valves on pipes to prevent water entering the home; or
4) Installed a pump to remove floodwaters that entered the home.

The implementation rate of dry floodproofing in France was found to range between 9.6 % (households that had installed a pump) and 36.1 % (households that had implemented any of the dry floodproofing measures). To determine which parameter settings resulted in a modeled implementation rate of floodproofing measures that reflected the implementation rate found by Poussin et al. (2013), Tierolf et al. (2023) explored the parameter space of parameter ranges found in the literature. The resulting parameter settings were also applied in this model (Table 2).

*Gravity mode*: Migration flows between inland regions and toward the coastal floodplain were calibrated on census data representing migration flows between departments by Tierolf et al. (2023). Migration flows were calibrated by fitting a gravity model on migration flow data following an ordinary least-squares regression (Benveniste et al., 2020), which yielded an R-squared of 0.71 (Tierolf et al., 2023). At present, data on SLR-induced migration in France is not available. Therefore, we could not calibrate the model based on observed SLR-induced migration. Considering this limitation, we focus our results on comparisons of climate and adaptation scenarios rather than a quantification of absolute migration numbers.

### 3.9. Sensitivity analysis

DYNAMO-M has previously been shown to be sensitive to changes in FPS and fixed migration costs (Tierolf et al., 2023). Here, we performed an additional one-at-a-time sensitivity analysis to assess the sensitivity to uncertainty in each new specification of beach amenity (50 % and 150 % of the values used to generate the main results) and the loss of flood protection after the disappearance of a sandy beach (beach loss reducing the flood protection to protection against flooding to one in two year recurrence intervals, and no loss of flood protection). We then compared the projected SLR-induced migration, development of coastal flood risk, and exposed population to the *standard* model settings described in the Method section.

**Table 2**
Calibrated parameter settings.

| Parameter | Value |
|---|---|
| *Peak risk perception* | 2 |
| *Loan duration* | 16 years |
| *Loan interest rate* | 4 % |
| *Expenditure cap* | 6 % |

## 4. Results

In this section, we present the mean results of 50 repetitive model runs per scenario. First, we present the modeled SLR-induced migration, the development of residential flood risk, and the uptake of dry floodproofing measures on a national scale. Next, we highlight our results for the three regions most affected by SLR. Then, we present cost estimates for beach renourishment and finally discuss the results of the sensitivity analysis.

### 4.1. Modeled SLR induced-migration and development of residential flood risk

Driven by population growth and coastward migration, the population residing in the coastal 1/100-flood zone increased from ~261,000 inhabitants in 2015 to ~450,000 and ~ 600,000 inhabitants in 2080 under *FullAdaptation* under SSP2–RCP4.5 and SSP5–RCP8.5, respectively (Supplementary Fig. S2). Panels *a* and *b* of Fig. 4 show the cumulative SLR-induced migration compared to the baseline under both SSP2–RCP4.5 and SSP5–RCP8.5 for each of the three adaptation scenarios (see methods). SLR drives migration under all adaptation settings. However, after 2050, large differences exist in the projected number of SLR-induced migrants between adaptation strategies. Without household and government adaptation to SLR (*NoAdaptation*), we project, by 2080, a cumulative net migration of 3.0 % (~13,100 people) or as much as 3.7 % (~21,700 people) of the population residing in the coastal flood zone under SSP2–RCP4.5 and SSP5–RCP8.5, respectively. Including household adaptation without beach renourishment (*HouseholdAdaptation*) slightly reduced this net migration to 2.6 % (~11,500 people) and 3.3 % (~20,000 people), respectively. Allowing for both household and government adaptation through renourishment (*FullAdaptation*) resulted in the least SLR induced migration, amounting to 2.0 % (~9100 people) under SSP2–RCP4.5 and 2.3 % (~13,800 people) under SSP5–RCP8.5. Compared to a scenario of no coastal adaptation to SLR, adaptation by households and governments reduced the total projected SLR induced migration in 2080 by 31 % and 36 % under SSP2-RCP4.5 and SSP5-RCP8.5, respectively. The slightly lower outmigration when also simulating household adaptation decisions in addition to household migration shows that households had a slight preference to remain and adapt compared to migrating. The larger decrease in outmigration when accounting for beach renourishment shows that renourishment could greatly reduce migration out of the coastal flood zone under SLR.

The development of residential flood risk over time is shown in panels *c* and *d* of Fig. 4. In a scenario of no coastal adaptation (*NoAdaptation*), flood risk expressed in expected annual damage increased from €162 million in 2015 to €1542 million and €2583 million in 2080 under SSP2–RCP4.5 and SSP5–RCP8.5, respectively. Modeling household adaptation (*HouseholdAdaptation*) lowered the 2080 projections to €1402 million and €2378 million. A scenario of household and government adaptation through beach renourishment (*FullAdaptation*) resulted in a projected flood risk of €1293 million and €2109 million in 2080 under SSP2–RCP4.5 and SSP5–RCP8.5, respectively. Compared to a scenario of no coastal adaptation, a combination of dry floodproofing and beach renourishment reduced flood risk by 16 % and 18 % in 2080 under SSP2–RCP4.5 and SSP5–RCP8.5, respectively. These results show that household adaptation and governmental protection schemes through beach renourishment could potentially lower coastal flood risk.

The large increase in coastal flood risk shown in Figs. 4c–d can be attributed to the combined effect of increasing asset value through GDP development, the increase in exposed population due to population growth and coastward migration, and SLR. Projections of the total population residing in the 1/100-year floodplain and the development of flood risk under a baseline scenario of no SLR are presented in Supplementary Fig. S2. Results for individual departments are provided in Supplementary Tables S1–S3.

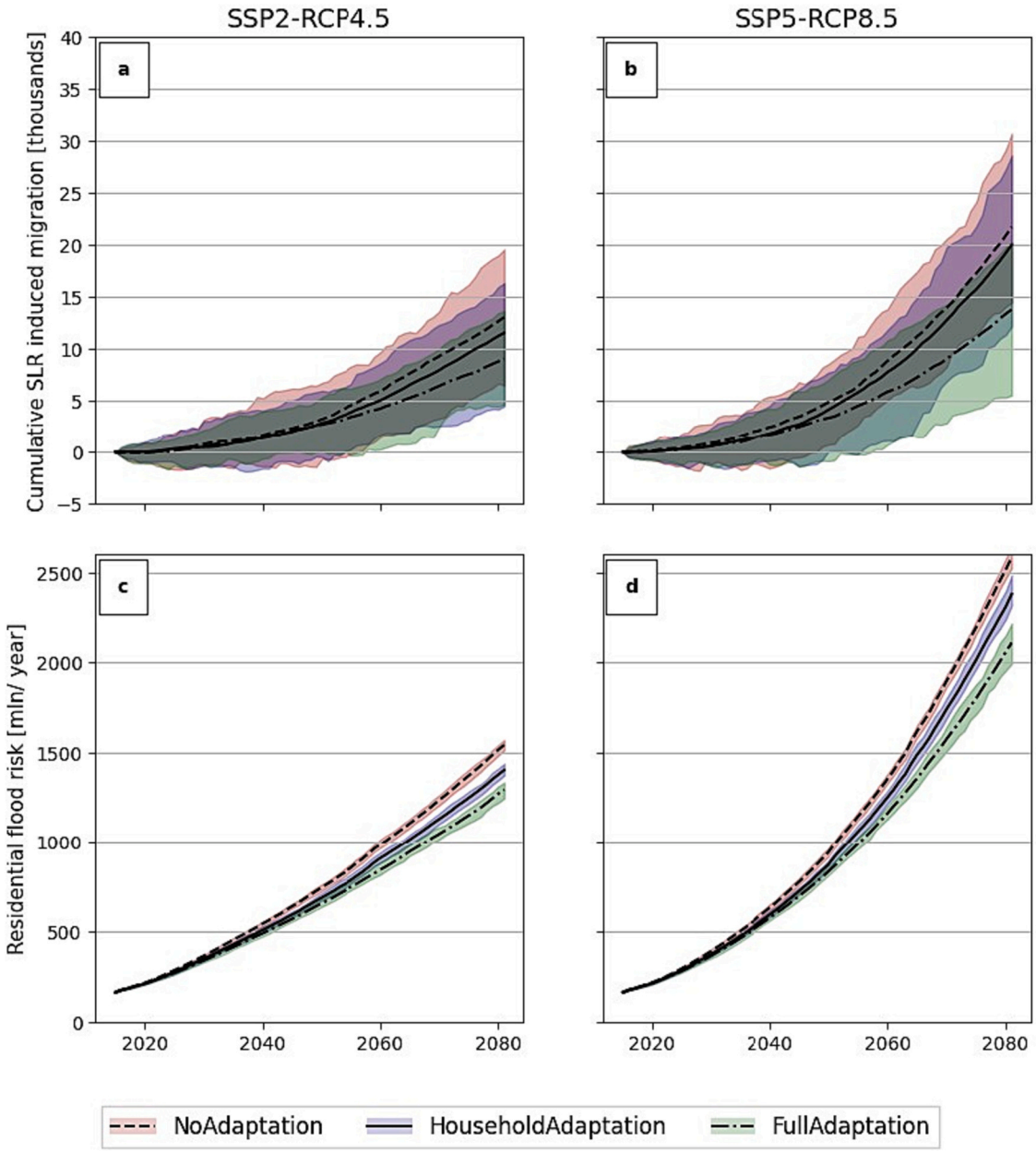


**Fig. 4.** Modeled cumulative SLR-induced migration between 2015 and 2080 (panels a and b) and the development of residential coastal flood risk (panels c and d) under three behavioral settings (*NoAdaptation*, *HouseholdAdaptation, FullAdaptation*) in the whole of France. Shadings indicate the lower and upper bounds of 50 repetitions per model run per behavioral scenario. Lines indicate the means of these runs. Each model run is initialized with a spin-up period of 15 years in which the *FullAdaptation* strategy was applied.

### 4.2. Implementation of dry floodproofing measures

Fig. 5 shows the development of the household implementation rate of dry floodproofing measures. SLR approximately doubles the implementation uptake of dry floodproofing under both the strategies of *HouseholdAdaptation* and *FullAdaptation*. Although the development of coastal flood risk is greatly affected by SSP and RCP projections (Fig. 4c–d), differences in socioeconomic development and SLR between the SSP–RCP scenarios did affect the implementation rate of dry floodproofing measures. Coastal protection through beach renourishment did not have an effect on the implementation rate of dry floodproofing; the implementation rate in both adaptation scenarios peaked around 20 % in 2080. This result might hint at a limit to household adaptation to flood risk. Through beach renourishment, households residing within 1 km of a sandy beach did not experience a loss in coastal flood protection, whereas flood protection for other households was maintained to flooding with 1 in 10 year recurrence intervals. Regional differences occurred in household uptake of adaptation measures (Fig. 6; Supplementary table S4). In this section, we present the results under SSP5–RCP8.5.

### 4.3. Regional adaptation and migration dynamics

Over 50 % of all SLR-induced migration occurred in three out of the 25 coastal departments (*Nor*, *Seine-Maritime*, and *Ille-et-Vilaine*, see Table 3). These departments saw high levels of migration due to the presence of major cities in the coastal floodplain (*Duinkerke* in *Nord* and *le Havre* in *Seine-Maritime*) and the extent of the coastal floodplain (in *Ille-et-Vilaine*), both of which resulted in a large population being exposed to coastal flooding (Supplementary Table S2).

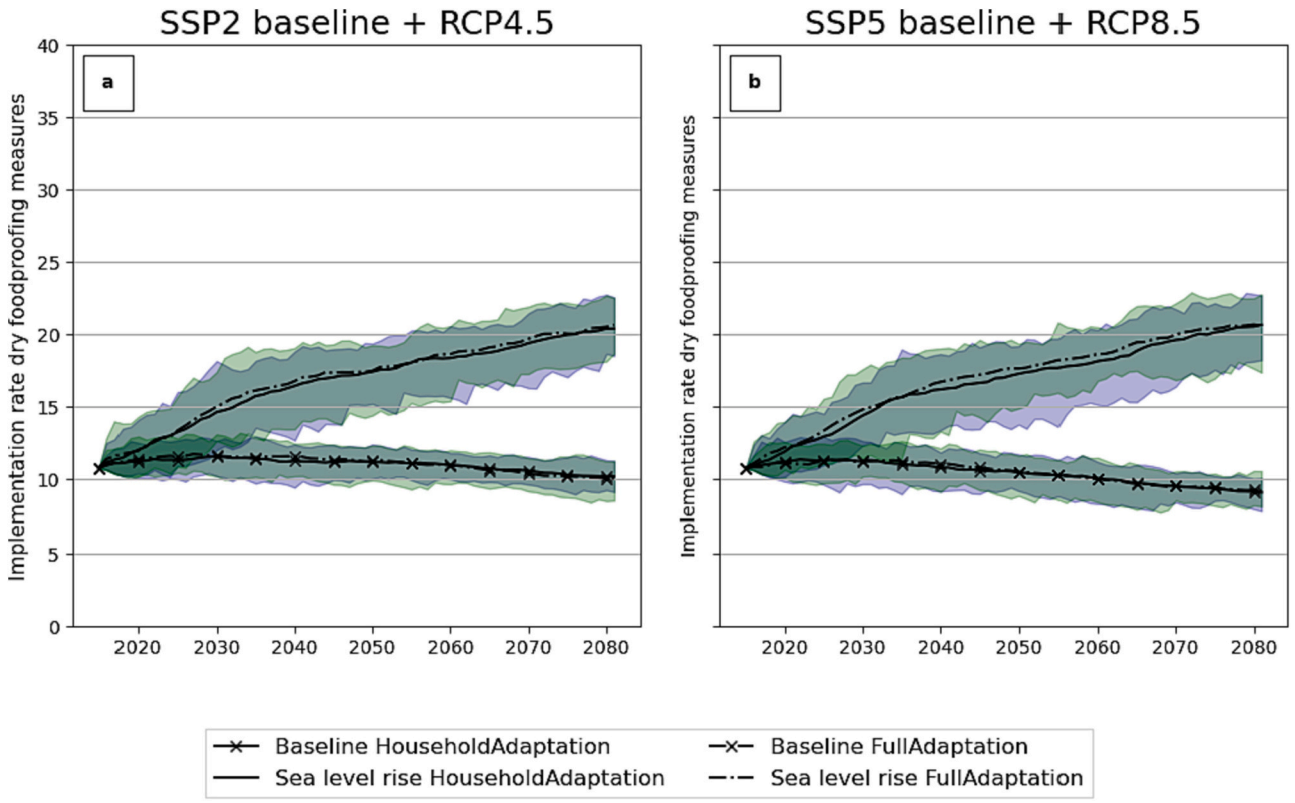


**Fig. 5.** The national household implementation rate of dry floodproofing measures. Panel a shows the percentage of households that had implemented dry floodproofing measures under SSP2 combined with a baseline scenario of no SLR, and with RCP4.5. Panel *b* shows the uptake of dry floodproofing measures under SSP5 combined with a baseline of no SLR and RCP8.5. The strategy of *NoAdaptation* is omitted from this figure, as households did not implement floodproofing measures under that strategy. Shading indicates the upper and lower bound of 50 repetitive runs, and lines indicate the mean of these runs.

We project nearly half of the SLR-induced migration to occur in *Nord*, where the cumulative SLR-induced migration up to 2080 under RCP8.5–SSP5 amounted to 7500 people under the *NoAdaptation* strategy and 7100 people under the *FullAdaptation* strategy (Fig. 6, in red). In this department, we project that ~112,000 people could inhabit the coastal floodplain in 2080, with 15 % of all households having implemented floodproofing measures. Beach renourishment was found to have the largest effect on reducing SLR-induced migration in absolute numbers in *Manche*, where it reduced the projected number of net migrations from ~1500 people under a *HouseholdAdaptation* to ~500 people under *FullAdaptation.* The simulated implementation of dry floodproofing measures was highest in *Bouches-du-Rhône*, located on the Mediterranean coast. In this region, we project a population of ~12,000 people residing in the coastal flood zone in 2080, with 66 % of all households having implemented floodproofing measures. Beach renourishment and household adaptation reduced SLR-induced migration from 200 people under *NoAdaptation* to 100 people under *FulAdaptation*. The development of coastal flood risk, adaptation uptake, and simulated population change for each coastal department under SSP2–RCP4.5 and SSP5–RCP8.5 are provided in Supplementary Tables S1–3.

### 4.4. Renourishment costs

The simulated beach renourishment volumes and costs are presented in Table 4. The total beach renourishment volume under a baseline scenario of no SLR (only accounting for ambient changes) amounted to 0.5 billion $m^3$ in 2080, with an annual average of 8 million $m^3$ of sand. Under RCP4.5, a total volume of 0.9 billion $m^3$ of sand was required to offset all erosion between 2015 and 2080. The annual fill volume increased to 13 million $m^3$/year in 2080. The total volume of sand required to offset erosion between 2015 and 2080 under RCP8.5 was 1.1 billion $m^3$, the annual renourishment volume required to offset erosion increased to 19 million $m^3$/year.

Assuming a cost of €7/$m^3$ sand in 2015, the total cost of beach renourishment under SSP2–RCP4.5 amounted to €13 billion, with the annual renourishment cost amounting to €270 million in 2080. The total renourishment cost under SSP5–RCP8.5 between 2015 and 2080 was €19 billion. Annual renourishment costs increased to €523 million in 2080. Annual beach renourishment volumes required to offset all erosion between 2015 and 2080 increased by a factor of 1.8 under RCP4.5 and a factor of 2.2 under RCP8.5. Accounting for SLR thus approximately doubled the volumes of sand required to maintain the current level of coastal flood protection of sandy beaches.

### 4.5. Sensitivity analysis

The sensitivity of projections of SLR-induced migration to different specifications of beach amenity value and FPS after beach erosion is shown in Table 5. SLR induced migration, total population residing in the coastal flood plain, and residential flood risk under both SSP2–RCP4.5 and SSP5–RCP8.5 are presented in Supplementary Tables S4–6, projections of flood risk and cumulative SLR-induced migration over time in Supplementary Fig. S3 and S4. In this section, we present the model sensitivity under SSP5-RCP8.5 to changes in coastal amenity value and beach flood protection.

*Beach amenity value*: Decreasing beach amenity value by 50 % resulted in less SLR-induced migration compared to standard model runs under the *HouseholdAdaptation* strategy, while the projected SLR-induced migration under the *NoAdaptation* and *FullAdaptation* strategies was comparable to the standard model runs. A lower amenity value resulted in a lower population in the floodplain and thus less flood risk under all RCP scenarios (see Supplementary Tables S6–7). Households in

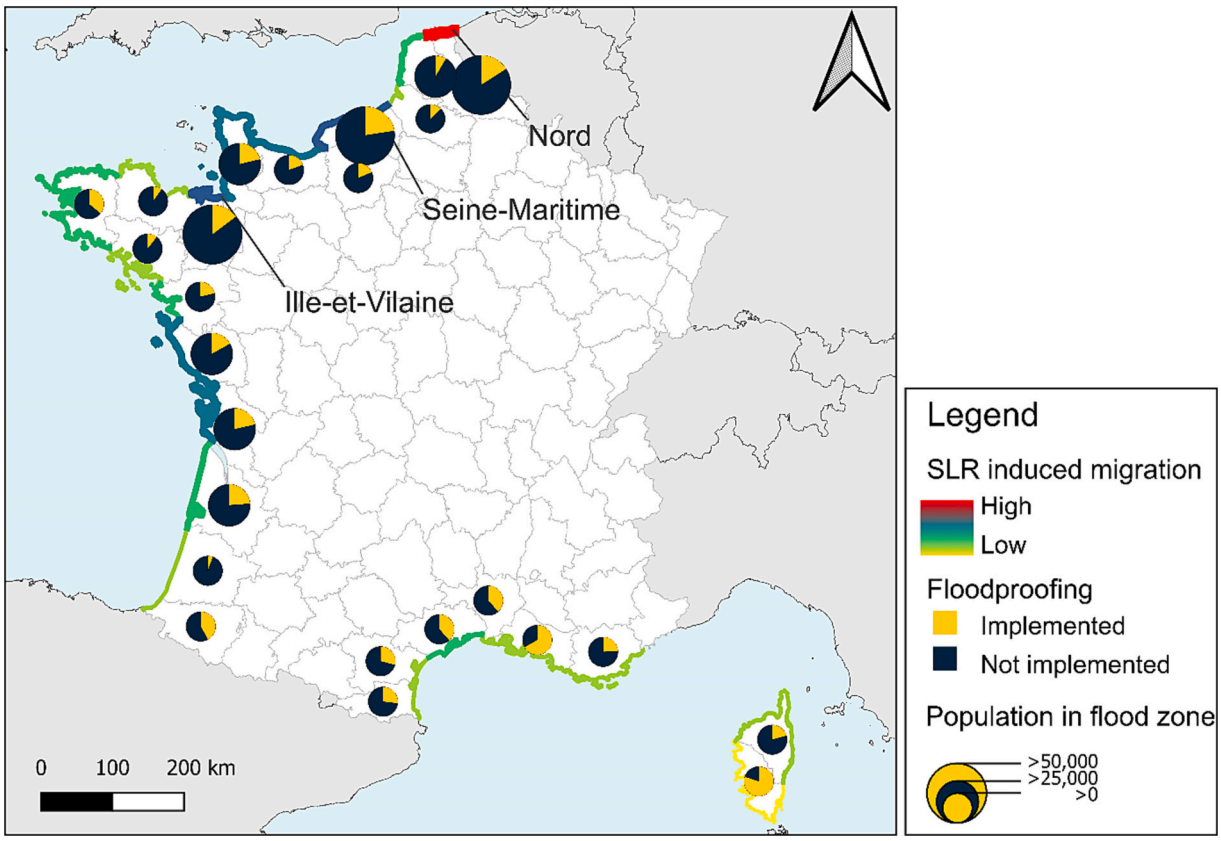


**Fig. 6.** Plotted adaptation uptake and SLR-induced migration under SSP5–RCP8.5 in 2080 considering a scenario of *HouseholdAdaptation*. Coastline segments indicate the relative amount of SLR-induced migrants per department and pie charts indicate the fraction of households that had implemented dry floodproofing measures. Pie charts are scaled relative to the total population residing in the coastal floodplain in 2080. Three regions, amounting to 50 % of all SLR-induced migration, are highlighted with labels.

**Table 3**
Total SLR-induced net outmigration by 2080 per coastal department under different coastal adaptation strategies and climate change scenarios. The table shows the mean result of 50 repetitive runs.

| Department | Adaptation scenario | | | | | |
|---|---|---|---|---|---|---|
| | NoAdaptation | | HouseholdAdaptation | | FullAdaptation | |
| | RCP4.5 | RCP8.5 | RCP4.5 | RCP8.5 | RCP4.5 | RCP8.5 |
| Nord | 4817 | 7557 | 4110 | 7631 | 3947 | 7082 |
| Seine-Maritime | 1106 | 1823 | 1313 | 1677 | 960 | 1180 |
| Ille-et-Vilaine | 967 | 1760 | 1040 | 1755 | 734 | 815 |
| Manche | 778 | 1690 | 754 | 1541 | 367 | 569 |
| Charente-Maritime | 859 | 1393 | 614 | 1043 | 207 | 392 |
| Calvados | 596 | 1246 | 470 | 1117 | 222 | 437 |
| Vendée | 491 | 1208 | 558 | 1197 | 618 | 504 |
| Pas-de-Calais | 890 | 1202 | 739 | 995 | 586 | 676 |
| Gironde | 616 | 1015 | 605 | 798 | 380 | 583 |
| Hérault | 612 | 709 | 417 | 654 | 432 | 698 |
| Finistère | 336 | 613 | 247 | 423 | 74 | 121 |
| Loire-Atlantique | 206 | 372 | 171 | 299 | 115 | 102 |
| Somme | 169 | 275 | 120 | 227 | 80 | 169 |
| Bouches-du-Rhône | 136 | 200 | 94 | 119 | 68 | 100 |
| Morbihan | 67 | 192 | 41 | 106 | 33 | 83 |
| Côtes-d'Armor | 112 | 141 | 84 | 106 | 83 | 79 |
| Eure | 53 | 101 | 44 | 79 | 71 | 96 |
| Gard | 71 | 92 | 70 | 81 | 64 | 57 |
| Haute-Corse | 36 | 50 | 31 | 50 | 23 | 35 |
| Var | 90 | 29 | −10 | 91 | −33 | 16 |
| Pyrénées-Atlantiques | 25 | 24 | 18 | 12 | 23 | 27 |
| Pyrénées-Orientales | 11 | 11 | 0 | 3 | −1 | 1 |
| Aude | 11 | 10 | 11 | 12 | 10 | 12 |
| Landes | 2 | 4 | 2 | 8 | 2 | 7 |
| Corse-du-Sud | 0 | −1 | −2 | −33 | −5 | −46 |

**Table 4**
Simulated beach renourishment volumes and costs under the *FullAdaptation* setting, results for SSP5–Baseline are presented within brackets.

| Scenario | Total fill volume ($10^9$ $m^3$) | Annual volume 2080 ($10^6$ $m^3$/ year) | Total cost 2080 ($10^9$ EUR) | Annual cost 2080 ($10^6$ EUR/ year) |
|---|---|---|---|---|
| SSP2(5)-Baseline | 0.5 | 8 | 8 (9) | 173 (226) |
| SSP2-RCP4.5 | 0.9 | 13 | 13 | 270 |
| SSP5-RCP8.5 | 1.1 | 19 | 19 | 523 |

**Table 5**
SLR-induced migration until 2080 considering different specifications of beach amenity value and coastal flood protection after beach erosion under SSP5–RCP8.5. Net outmigration is shown in absolute numbers and as a percentage of the population residing the coastal in floodplain in 2080 under a baseline scenario of no SLR.

| | NoAdaptation | HouseholdAdaptation | FullAdaptation |
|---|---|---|---|
| Standard | 21,700 (3.7 %) | 20,000 (3.3 %) | 13,800 (2.3 %) |
| Low beach amenity (50 %) | 22,000 (3.8 %) | 17,100 (2.9 %) | 14,700 (2.5 %) |
| High beach amenity (150 %) | 22,800 (3.9 %) | 20,300 (3.4 %) | 12,500 (2.1 %) |
| No loss of flood protection | 19,300 (3.3 %) | 16,800 (2.8 %) | 14,300 (2.4 %) |
| Greater loss of flood protection | 27,400 (4.7 %) | 23,000 (3.9 %) | 14,300 (2.4 %) |

this setting were less likely to settle or stay in areas of high flood risk, as the beach amenity value no longer offsets perceived flood risk. Under the *HouseholdAdaptation* strategy, in these less hazardous areas, the benefits of adaptation more often outweighed the benefits of migration, increasing the effect of household adaptation on migration decisions. The trade-off between coastal amenities and flood risk is also illustrated by differences in expected annual damages (Supplementary Table S6). A lower beach amenity value resulted in less coastal flood risk, whereas a higher beach amenity value resulted in a higher coastal flood risk under all adaptation strategies.

*Flood protection sandy beaches*: The model proved to be more sensitive to uncertainty in specifications of the loss of flood protection after a beach had completely eroded. Not accounting for a loss of flood protection resulted in less migration under *NoAdaptation* and *HouseholdAdaptation,* whereas no effect on migration occurred under *FullAdaptation* (Table 5). Under this setting, differences in coastal net outmigration under *NoAdaptation* and *HouseholdAdaptation* compared to *FullAdaptation* were driven only by differences in beach amenity values. This indicates that without a loss of flood protection, beach renourishment would still result in less SLR-induced migration. Maintaining wider beaches under *FullAdaptation* increased the amenity value (attractiveness) of living near the coast, offsetting the perceived coastal flood risk in the utility-based migration decisions.

Simulations with a greater loss of coastal flood protection resulted in more migration under *NoAdaptation* and *HouseholdAdaptation* and increased the effect of beach renourishment (*FullAdaptation*) on migration decisions when compared to standard model settings (Table 5). This result indicates that beach renourishment could reduce SLR-induced migration by maintaining the natural flood protection offered by sandy beaches.

## 5. Discussion

Research interest in modeling the adaptation and migration behavior of coastal communities affected by the impacts of SLR is growing (Bell et al., 2021; Hauer, 2017; Hinkel et al., 2013; Lincke and Hinkel, 2021). In this study, we contribute to this topic by integrating spatially explicit projections of SLR and shoreline change in an ABM (DYNAMO-M) simulating household behavior under coupled socioeconomic and climate change scenarios (de Ruig et al., 2022; Haer et al., 2019; Luijendijk et al., 2018; Tierolf et al., 2023; Vousdoukas et al., 2020). By explicitly simulating interactions between governmental protection schemes (beach renourishment) and household decisions (floodproofing and migration) we hereby provide a "bottom up" representation of coastal adaptation and migration dynamics (Horton et al., 2021).

We find that SLR induced-migration is affected by coastal adaptation; the combination of household adaptation to flood risk and beach renourishment reduces the projected SLR-induced migration by up to 36 %. Through a comparison of migration rates under a scenario with and without household adaptation to flooding, we show that households preferred staying and implementing adaptation measures instead of opting to migrate. This result aligns with Duijndam et al.'s (2023) findings of that governmental support for local household adaptation to flood risk could reduce SLR-induced migration. We find that government protection schemes through beach renourishment could further reduce SLR-induced migration; maintaining beach width affects household decisions through reduced coastal flood risk and increased amenity values. The effectiveness of beach renourishment in mitigating flood damage and coastal retreat has also been discussed by Houston. (2022), who argues that beach renourishment is an attractive strategy for protecting developed shorelines. For example, an analysis of Hurricane Sandy showed that renourishment projects saved an estimated $1.3 billion in avoided infrastructural damages, whereas the cost of the renourishment project could easily be offset by tax returns through increased tourism revenue (Army Corps of Engineers, 2016; Houston., 2022).

Without accounting for household adaptation and beach renourishment, we find that SLR and coastal erosion could result in a net outmigration of between 13,100–21,700 residents living in the coastal floodplain by 2080. Over 50 % of this migration is expected to occur in three out of the 25 coastal departments. These estimates are low compared to the findings of Lincke and Hinkel (2021), who found that in France, SLR could drive the migration of 54,006–386,274 people by 2100 under the same SSP–RCP combinations. Part of this difference can be explained by how migration decision is modeled. Lincke and Hinkel (2021) assumed that households that reside in the 1/1-year floodplain would migrate autonomously if a cost–benefit analysis deemed coastal protection measures not to be the optimal strategy for the coastal segment they reside in. This assumption resulted in the immediate migration of the population currently residing in the 1/1-year floodplain protected by dikes that were not included in their model. We assumed that all areas will be protected by a FPS of 1/10 years until 2080, except in areas where beaches are lost. This comparison again highlights the effect of assumptions on flood protection infrastructure on projections of SLR-induced migration.

We assumed that the government in France would continuously increase dike heights to maintain the initial coastal FPS of 1/10 years for all coastal regions. However, the upgrading of existing flood infrastructure in sparsely populated areas might not be justified, whereas investments in flood protection could prove beneficial in more densely populated urban areas (Hinkel et al., 2018; Nicholls et al., 2019). Assuming that an FPS of 1/10 years is maintained in the whole of France could result in underestimations of SLR-induced migration in areas of low population density and severe overestimations of migration in densely populated urban areas, as projections of SLR-induced migration largely depend on the FPS assumed in the model (Tierolf et al., 2023). An interesting further development of the model could include the implementation of a regional cost–benefit analysis of investments in flood protection infrastructure. Regions in which FPS are no longer maintained could see an increase in SLR-induced migration or the implementation rate of dry floodproofing measures.

We found that projections of SLR-induced migration were highly sensitive to change in the assumed flood protection offered by sandy beaches. We assumed protection to only be lost once the shoreline had retreated by >100 m since 2015 and that the loss of flood protection would only affect households residing within 1 km of the beach. We also did not account for increased inundation depth or flood extent due to dune erosion and changes in beach profile, possibly underestimating the effect of coastal erosion on flood severity. Since Toimil et al. (2023) found that the effect of uncertainty in erosion processes on inundation depth and extent to be greater than that of uncertainty in the rate of SLR, a more detailed modeling of the interactions between beach erosion and coastal flood hazards may benefit projections of SLR-induced migration, as the loss of sandy beaches may affect communities located further from the shoreline than accounted for in this model.

The annual volume of beach renourishment when only including ambient shoreline change was much higher than the historical annual fill volume found in the literature (8 million $m^3$/year compared to 0.7 million $m^3$/year found by Hanson et al., 2002). The difference in annual fill volumes may in part result from the low number of beach renourishment projects recorded before 2002, as more recent overviews of beach renourishment practice in Europe are, to the best of our knowledge, currently nonexistent. However, it could also be attributed to beaches migrating inland while maintaining beach width, a process that is not considered in this study (Cooper et al., 2020; Luijendijk et al., 2018). Since historical ambient shoreline change is projected into the future, a potential overestimation of beach loss has implications for renourishment volumes. When accounting for SLR, the annual fill rate increased to up to 19 million $m^3$/year, with annual renourishment costs of €523 million/year in 2080. Estimates of the beach renourishment costs associated with SLR would benefit from a more detailed modeling of coastal shoreline change dynamics.

## 6. Conclusions and recommendations

In this study, we simulated coastal adaptation dynamics in France in the face of SLR using DYNAMO-M. We further develop this ABM to include coastal erosion and beach renourishment and simulate household decisions under coupled SSPs and RCPs. By explicitly modeling household behavior combined with governmental protection strategies under increasing coastal risks, the new model framework presented in this study allows for a comparison of climate change impacts on coastal communities under different adaptation strategies. Results indicate that without any local adaptation, SLR could drive the cumulative net migration of 13,100 and 21,700 people between 2015 and 2080 under SSP2–RCP4.5 and SSP5–RCP8.5, respectively, which amounted to 3.0 % and 3.7 % of the coastal population residing in the 1/100-year flood zone in 2080 under a scenario of no SLR. Coastal adaptation to SLR through renourishment combined with floodproofing lowered this projected SLR-induced migration by up to 37 %. Expected annual flood damages were projected to increase from €162 million in 2015, to up to €1542 million and €2583 million in 2080 under SSP2–RCP4.5 and SSP5–RCP8.5, respectively. Coastal adaptation by floodproofing homes and beach renourishment decreased these estimates of future flood risk to €1293 million and €2109 million, respectively.

Although the number of beach renourishment projects in France is increasing (Pranzini et al., 2015), our results indicate that much potential still exists for beach renourishment to reduce both coastal flood risk and SLR-induced migration. However, beach renourishment could have detrimental impacts on coastal ecosystems (Speybroeck et al., 2006). Increased turbidity caused by dredging activities could smother nearshore ecosystems, and changes in sediment composition in the deposition sites could affect species abundance (Saengsupavanich et al., 2023). The impacts of sediment extraction and renourishment activities are not yet fully understood, and monitoring strategies are often underdeveloped (Peterson and Bishop, 2005). Combined with the reliance of renourishment on periodic replenishment from a limited number of borrow sites, this may deem beach renourishment an unsustainable adaptation strategy in some areas. The implementation of beach renourishment projects should be evaluated on a site-by-site basis, considering both benefits in terms of flood protection and coastal attractiveness as well as potential negative effects on local coastal ecosystems.

The modeled implementation rate of dry floodproofing measures by households increased with SLR; however, it did not exceed 20 % under either RCP4.5 or RCP8.5. This result indicates economical and societal limits to household adaptation in France (Adger et al., 2009). Factors constraining adaptation uptake are risk perceptions and budget constraints (Hudson, 2020; Poussin et al., 2014). Financial support combined with risk education may increase the household implementation rate of floodproofing measures, which could further reduce coastal flood risk, allowing households to remain in the floodplain for longer under SLR.

Another limitation is the lack of disaggregated data on flood protection infrastructure in France. In this study, we assumed a constant FPS of 1/10-years throughout the whole of France, whereas in reality, densely populated urban areas may be protected from flooding of return periods of up to 1/100-years (Tourment et al., 2018). Modeling efforts would benefit from spatially disaggregated information on flood protection infrastructure. The FLOPROS dataset constructed by Scussolini et al. (2016) aims to provide an overview of FPS on a subnational scale; however, the construction of such databases is hampered by the lack of centralized national databases on flood protection infrastructure. In the absence of this data, a cost–benefit analysis of investments in flood protection infrastructure considering future population development could provide insights into which areas will be protected in the future (Lincke and Hinkel, 2018; Tiggeloven et al., 2020).

We acknowledge that migration decisions in the face of SLR are multifaceted. We therefore modeled household migration not only based on perceived flood risk but also considering wealth, income differentials, coastal amenity values, and government protection schemes (Black et al., 2011; Hauer et al., 2020). A more realistic representation of household behavior could be achieved by, for example, distinguishing between age groups. Schaffar et al. (2019) found that in France, retirees leave large urban areas, such as the Paris agglomeration, to move to more rural coastal zones with preferable climates. Including these dynamics in ABMs of population responses to SLR could potentially affect migration rates, as the demographic composition could affect future climate mobility in the coastal flood zone (Hugo, 2011). Further development could also include social networks inside and outside of the household's place of residence. The presence and strength of these networks were shown to affect migration intentions in response to SLR (Duijndam et al., 2023). Altering the psychological costs of migration based on the presence, strength, and change of social networks in origin and destination regions could be an interesting further development of DYNAMO-M. Other improvements can be made by calibrating risk perceptions and migration preferences based on more localized survey data, thereby better incorporating empirical findings into the modeling research (Duijndam et al., 2022).

In addition to prompting migration through increasing coastal flood hazards and shoreline change, SLR also influences coastal migration by exacerbating saltwater intrusion (Hauer et al., 2020). In future research, the modeling approach described in this study could be further developed to provide projections of SLR-induced migration considering the combined effect of increasing storm surge frequency and severity, coastal erosion, and saltwater intrusion on household decisions.

## Code availability statement

All model code is available from https://github.com/ltierolf/DYNAMO-M and doi:https://doi.org/10.5281/zenodo.7656577.

## CRediT authorship contribution statement

**Lars Tierolf:** Writing – review & editing, Writing – original draft, Visualization, Methodology, Investigation, Formal analysis, Conceptualization. **Toon Haer:** Writing – review & editing, Supervision, Methodology, Conceptualization. **Panagiotis Athanasiou:** Writing – review & editing, Methodology, Conceptualization. **Arjen P. Luijendijk:** Writing – review & editing, Methodology, Conceptualization. **W.J. Wouter Botzen:** Writing – review & editing, Supervision, Methodology, Conceptualization. **Jeroen C.J.H. Aerts:** Writing – review & editing, Supervision, Project administration, Methodology, Conceptualization.

## Declaration of competing interest

The authors declare that they have no known competing financial interests or personal relationships that could have appeared to influence the work reported in this paper.

## Data availability

All input data used in this model can be obtained from the original data sources described in the methodology.

## Acknowledgements

This study has been conducted under the EU ERC COASTMOVE grant nr. 884442 (www.coastmove.org).

## Appendix A. Supplementary data

Supplementary data to this article can be found online at https://doi.org/10.1016/j.scitotenv.2024.170239.

## References

Adger, W.N., Dessai, S., Goulden, M., Hulme, M., Lorenzoni, I., Nelson, D.R., Naess, L.O., Wolf, J., Wreford, A., 2009. Are there social limits to adaptation to climate change? Clim. Chang. 93 (3), 335–354. https://doi.org/10.1007/s10584-008-9520-z.

Aerts, J.C.J.H., 2018. A review of cost estimates for flood adaptation. In: Water (Switzerland), vol. 10, Issue 11. MDPI AG, p. 1646. https://doi.org/10.3390/w10111646.

Aerts, J.C.J.H., Botzen, W.J.W., Emanuel, K., Lin, N., de Moel, H., Michel-Kerjan, E.O., 2014. Evaluating flood resilience strategies for coastal megacities. Science 344 (6183), 473–475. https://doi.org/10.1126/science.1248222.

Aerts, J.C.J.H., Barnard, P.L., Botzen, W., Grifman, P., Hart, J.F., De Moel, H., Mann, A. N., de Ruig, L.T., Sadrpour, N., 2018. Pathways to resilience: adapting to sea level rise in Los Angeles. Ann. N. Y. Acad. Sci. 1427 (1), 1–90. https://doi.org/10.1111/nyas.13917.

Anderson, J.E., 2011. The gravity model. Annual Review of Economics 3, 133–160. https://doi.org/10.1146/annurev-economics-111809-125114.

Anthony, E.J., 1997. The status of beaches and shoreline development options on the French Riviera: a perspective and a prognosis. J. Coast. Conserv. 3 (2), 169–178.

Army Corps of Engineers, 2016. Messages in the sand from Hurricane Sandy. DVIDS. https://www.dvidshub.net/news/208990/messages-sand-hurricane-sandy.

Athanasiou, P., van Dongeren, A., Giardino, A., Vousdoukas, M., Gaytan-Aguilar, S., Ranasinghe, R., 2019. Global distribution of nearshore slopes with implications for coastal retreat. Earth System Science Data 11 (4), 1515–1529. https://doi.org/10.5194/essd-11-1515-2019.

Athanasiou, P., van Dongeren, A., Giardino, A., Vousdoukas, M.I., Ranasinghe, R., Kwadijk, J., 2020. Uncertainties in projections of sandy beach erosion due to sea level rise: an analysis at the European scale. Sci. Rep. 10(1), Article 1 https://doi.org/10.1038/s41598-020-68576-0.

Audère, M., Robin, M., 2021. Assessment of the vulnerability of sandy coasts to erosion (short and medium term) for coastal risk mapping (Vendée, W France). Ocean Coast. Manag. 201, 105452 https://doi.org/10.1016/j.ocecoaman.2020.105452.

Barraqué, B., Moatty, A., 2020. The French Cat' Nat' system: post-flood recovery and resilience issues. Environmental Hazards 19 (3), 285–300. https://doi.org/10.1080/17477891.2019.1696738.

Bell, A.R., Wrathall, D.J., Mueller, V., Chen, J., Oppenheimer, M., Hauer, M., Adams, H., Kulp, S., Clark, P.U., Fussell, E., Magliocca, N., Xiao, T., Gilmore, E.A., Abel, K., Call, M., Slangen, A.B.A., 2021. Migration towards Bangladesh coastlines projected to increase with sea-level rise through 2100. Environ. Res. Lett. 16 (2), 024045 https://doi.org/10.1088/1748-9326/abdc5b.

Benavente, J., Del Río, L., Gracia, F.J., Martínez-del-Pozo, J.A., 2006. Coastal flooding hazard related to storms and coastal evolution in Valdelagrana spit (Cadiz bay Natural Park, SW Spain). Cont. Shelf Res. 26 (9), 1061–1076. https://doi.org/10.1016/j.csr.2005.12.015.

Benveniste, H., Oppenheimer, M., Fleurbaey, M., 2020. Effect of border policy on exposure and vulnerability to climate change. Proc. Natl. Acad. Sci. 117 (43), 26692–26702. https://doi.org/10.1073/pnas.2007597117.

Bird, E., Lewis, N., 2015a. Beach Renourishment. Springer International Publishing. https://doi.org/10.1007/978-3-319-09728-2.

Bird, E., Lewis, N., 2015b. Beach renourishment for coast protection. In: Bird, E., Lewis, N. (Eds.), Beach Renourishment. Springer International Publishing, pp. 101–106. https://doi.org/10.1007/978-3-319-09728-2_5.

Black, R., Bennett, S.R.G., Thomas, S.M., Beddington, J.R., 2011. Migration as adaptation. Nature. https://doi.org/10.1038/478477a.

Bombardini, M., Trebbi, F., 2012. Risk aversion and expected utility theory: an experiment with large and small stakes. J. Eur. Econ. Assoc. 10 (6), 1348–1399. https://doi.org/10.1111/J.1542-4774.2012.01086.X.

Bruun, P., 1962. Sea-level rise as a cause of shore erosion. Journal of the Waterways and Harbors Division 88 (1), 117–130. https://doi.org/10.1061/JWHEAU.0000252.

Chadenas, C., Creach, A., Mercier, D., 2014. The impact of storm Xynthia in 2010 on coastal flood prevention policy in France. *Source*. J. Coast. Conserv. 18 (5), 529–538. https://doi.org/10.1007/s.

Conroy, S.J., Milosch, J.L., 2011. An estimation of the coastal premium for residential housing prices in San Diego County. J. Real Estate Financ. Econ. 42 (2), 211–228. https://doi.org/10.1007/S11146-009-9195-X/TABLES/3.

Cooper, J.A.G., Masselink, G., Coco, G., Short, A.D., Castelle, B., Rogers, K., Anthony, E., Green, A.N., Kelley, J.T., Pilkey, O.H., Jackson, D.W.T., 2020. Sandy beaches can survive sea-level rise. In: Nature Climate Change, Vol. 10, Issue 11. Nature Publishing Group, pp. 993–995. https://doi.org/10.1038/s41558-020-00934-2.

Crapoulet, A., Héquette, A., Levoy, F., Bretel, P., 2016. Using LiDAR topographic data for identifying coastal areas of northern France vulnerable to sea-level rise. J. Coast. Res. 75 (sp1), 1067–1071. https://doi.org/10.2112/SI75-214.1.

Czembrowski, P., Kronenberg, J., 2016. Hedonic pricing and different urban green space types and sizes: insights into the discussion on valuing ecosystem services. Landsc. Urban Plan. 146, 11–19. https://doi.org/10.1016/j.landurbplan.2015.10.005.

Plan de Prévention des Risques Naturels Prévisibles Littoraux. DDTM 85, 2015. https://www.vendee.gouv.fr/IMG/pdf/RAP_PPRL-PaysOlonne_NotePresentation.pdf.

De Koning, K., Filatova, T., 2020. Repetitive floods intensify outmigration and climate gentrification in coastal cities. Environ. Res. Lett. https://doi.org/10.1088/1748-9326/ab6668.

de Ruig, L.T., Haer, T., de Moel, H., Brody, S.D., Botzen, W.J.W., Czajkowski, J., Aerts, J. C.J.H., 2022. How the USA can benefit from risk-based premiums combined with flood protection. Nat. Clim. Chang. 1–4 https://doi.org/10.1038/s41558-022-01501-7.

de Ruig, L.T., Haer, T., de Moel, H., Orton, P., Botzen, W.J.W., Aerts, J.C.J.H., 2023. An agent-based model for evaluating reforms of the National Flood Insurance Program: a benchmarked model applied to Jamaica Bay. NYC. Risk Analysis 43 (2), 405–422. https://doi.org/10.1111/risa.13905.

Dean, R.G., Houston, J.R., 2016. Determining shoreline response to sea level rise. Coast. Eng. 114, 1–8. https://doi.org/10.1016/j.coastaleng.2016.03.009.

Deboudt, P., 2010. Towards coastal risk management in France. Ocean Coast. Manag. 53 (7), 366–378. https://doi.org/10.1016/j.ocecoaman.2010.04.013.

Di Baldassarre, G., Viglione, A., Carr, G., Kuil, L., Salinas, J.L., Blöschl, G., 2013. Socio-hydrology: Conceptualising human-flood interactions. Hydrol. Earth Syst. Sci. 17 (8), 3295–3303. https://doi.org/10.5194/hess-17-3295-2013.

Duijndam, S.J., Botzen, W.J.W., Hagedoorn, L.C., Aerts, J.C.J.H., 2022. Anticipating sea-level rise and human migration: a review of empirical evidence and avenues for future research. WIREs Climate Change 13 (1), e747. https://doi.org/10.1002/wcc.747.

Duijndam, S.J., Botzen, W.J.W., Hagedoorn, L.C., Bubeck, P., Haer, T., Pham, M., Aerts, J.C.J.H., 2023. Drivers of migration intentions in coastal Vietnam under increased flood risk from sea level rise. Clim. Chang. 176 (2), 12. https://doi.org/10.1007/s10584-022-03479-9.

Durand, P., Anselme, B., Defossez, S., Elineau, S., Gherardi, M., Goeldner-Gianella, L., Longépée, E., Nicolae-Lerma, A., 2018. Coastal flood risk: improving operational response, a case study on the municipality of Leucate, Languedoc. France. Geoenvironmental Disasters 5 (1), 19. https://doi.org/10.1186/s40677-018-0109-1.

Eurostat, 2020. Income, consumption and wealth—experimental statistics (icw). In *European Statistical System (ESS)*. https://ec.europa.eu/eurostat/web/experimental-statistics/income-consumption-wealth.

Evans, D.J., Sezer, H., 2005. Social discount rates for member countries of the European Union. J. Econ. Stud. 32 (1), 47–59. https://doi.org/10.1108/01443580510574832.

FEMA. (2021). Requirements for the Design and Certification of Dry Floodproofed Non-Residential and Mixed-Use BuildingsResidential Floodproofing-Requirements and Certification for Buildings Located in Special Flood Hazard Areas in Accordance with the National Flood Ins. https://www.fema.gov/media-library/.

Fishburn, P.C., 1981. Subjective expected utility: a review of normative theories. Theory and Decision 1981 13:2 13 (2), 139–199. https://doi.org/10.1007/BF00134215.

Gopalakrishnan, S., Smith, M.D., Slott, J.M., Murray, A.B., 2011. The value of disappearing beaches: a hedonic pricing model with endogenous beach width. J. Environ. Econ. Manag. 61 (3), 297–310. https://doi.org/10.1016/J.JEEM.2010.09.003.

Haer, T., Botzen, W.J.W., de Moel, H., Aerts, J.C.J.H., 2017. Integrating household risk mitigation behavior in flood risk analysis: an agent-based model approach. Risk Anal. 37 (10), 1977–1992. https://doi.org/10.1111/risa.12740.

Haer, T., Botzen, W.J.W., Aerts, J.C.J.H., 2019. Advancing disaster policies by integrating dynamic adaptive behaviour in risk assessments using an agent-based

modelling approach. Environ. Res. Lett. 14 (4) https://doi.org/10.1088/1748-9326/ab0770.
Hanson, H., Brampton, A., Capobianco, M., Dette, H.H., Hamm, L., Laustrup, C., Lechuga, A., Spanhoff, R., 2002. Beach nourishment projects, practices, and objectives—a European overview. Coast. Eng. 47 (2), 81–111. https://doi.org/10.1016/S0378-3839(02)00122-9.
Hauer, M.E., 2017. Migration induced by sea-level rise could reshape the US population landscape. Nat. Clim. Chang. https://doi.org/10.1038/nclimate3271.
Hauer, M.E., Fussell, E., Mueller, V., Burkett, M., Call, M., Abel, K., McLeman, R., Wrathall, D., 2020. Sea-level rise and human migration. Nature Reviews Earth & Environment. https://doi.org/10.1038/s43017-019-0002-9.
Hinkel, J., Nicholls, R.J., Tol, R.S.J., Wang, Z.B., Hamilton, J.M., Boot, G., Vafeidis, A.T., McFadden, L., Ganopolski, A., Klein, R.J.T., 2013. A global analysis of erosion of sandy beaches and sea-level rise: an application of DIVA. Glob. Planet. Chang. 111, 150–158. https://doi.org/10.1016/j.gloplacha.2013.09.002.
Hinkel, J., Aerts, J.C.J.H., Brown, S., Jiménez, J.A., Lincke, D., Nicholls, R.J., Scussolini, P., Sanchez-Arcilla, A., Vafeidis, A., Addo, K.A., 2018. The ability of societies to adapt to twenty-first-century sea-level rise. Nature Climate Change 2018 8:7 8 (7), 570–578. https://doi.org/10.1038/s41558-018-0176-z.
Horton, R.M., de Sherbinin, A., Wrathall, D., Oppenheimer, M., 2021. Assessing human habitability and migration. Science 372 (6548), 1279–1283. https://doi.org/10.1126/science.abi8603.
Houston, J.R., 2017. Shoreline change in response to sea-level rise on Florida's west coast. J. Coast. Res. 33 (6), 1243–1260. https://doi.org/10.2112/JCOASTRES-D-17-00024.1.
Houston., 2022. Beach nourishment provides resilient protection for critical coastal infrastructure. Shore & Beach 19–32. https://doi.org/10.34237/1009023.
Hudson, P., 2018. A comparison of definitions of affordability for flood risk adaption measures: a case study of current and future risk-based flood insurance premiums in Europe. Mitig. Adapt. Strateg. Glob. Chang. 23 (7), 1019–1038. https://doi.org/10.1007/s11027-017-9769-5.
Hudson, P., 2020. The affordability of flood risk property-level adaptation measures. Risk Anal. 40 (6), 1151–1167. https://doi.org/10.1111/risa.13465.
Hugo, G., 2011. Future demographic change and its interactions with migration and climate change. Glob. Environ. Chang. 21, S21–S33. https://doi.org/10.1016/j.gloenvcha.2011.09.008.
Huizinga, J., de Moel, H., & Szewczyk, W. (2017). Global flood depth-damage functions. Methodology and the database with guidelines. In *Joint Research Centre (JRC)*. Joint Research Centre (Seville site). https://ec.europa.eu/jrc%0Ahttp://publications.jrc.ec.europa.eu/repository/bitstream/JRC105688/global_flood_depth-damage_functions_10042017.pdf.
INSEE. (2017). Structure et distribution des revenus, inégalité des niveaux de vie en 2014 | Insee. https://www.insee.fr/fr/statistiques/3560118 https://www.insee.fr/fr/statistiques/3126151.
Jackson, L.P., Jevrejeva, S., 2016. A probabilistic approach to 21st century regional sea-level projections using RCP and high-end scenarios. Glob. Planet. Chang. 146, 179–189. https://doi.org/10.1016/j.gloplacha.2016.10.006.
Jevrejeva, S., Grinsted, A., Moore, J.C., 2014. Upper limit for sea level projections by 2100. Environ. Res. Lett. 9 (10), 104008 https://doi.org/10.1088/1748-9326/9/10/104008.
Kennan, J., Walker, J.R., 2011. The effect of expected income on individual migration decisions. Econometrica 79 (1), 211–251. https://doi.org/10.3982/ecta4657.
Klabunde, A., Willekens, F., 2016. Decision-making in agent-based models of migration: state of the art and challenges. Eur. J. Popul. https://doi.org/10.1007/s10680-015-9362-0.
Koerth, J., Vafeidis, A.T., Hinkel, J., 2017. Household-level coastal adaptation and its drivers: a systematic case study review. Risk Anal. 37 (4), 629–646.
Kriebel, D.L., Dean, R.G., 1993. Convolution method for time-dependent beach-profile response. J. Waterw. Port Coast. Ocean Eng. 119 (2), 204–226. https://doi.org/10.1061/(ASCE)0733-950X(1993)119:2(204).
Kunreuther, H., 1996. Mitigating disaster losses through insurance. J. Risk Uncertain. 12 (2), 171–187. https://doi.org/10.1007/BF00055792.
Landry, C.E., Turner, D., Allen, T., 2022. Hedonic property prices and coastal beach width. Appl. Econ. Perspect. Policy 44 (3), 1373–1392. https://doi.org/10.1002/AEPP.13197.
Lincke, D., Hinkel, J., 2018. Economically robust protection against 21st century sea-level rise. Glob. Environ. Chang. 51, 67–73. https://doi.org/10.1016/j.gloenvcha.2018.05.003.
Lincke, D., Hinkel, J., 2021. Coastal migration due to 21st century sea-level rise. Earth's. Future 9 (5), e2020EF001965. https://doi.org/10.1029/2020EF001965.
Lins-de-Barros, F.M., Sauzeau, T., Guerra, J.V., 2019. Historical evolution of seafront occupation in France (Bay of Biscay) and Brazil (Rio de Janeiro) face to coastal erosion vulnerability and risks (19th—21th centuries). Confins 39. https://doi.org/10.4000/confins.18175.
Luijendijk, A., Hagenaars, G., Ranasinghe, R., Baart, F., Donchyts, G., Aarninkhof, S., 2018. The state of the World's beaches. Sci. Rep. 8 (1), 1–11. https://doi.org/10.1038/s41598-018-24630-6.
Marchand, M., Crosato, A., Klijn, F., 2006. Flood risk analysis for the river Scheldt estuary. https://www.waterbouwkundiglaboratorium.be/nl/open-wl-archief.
Maspataud, A., Ruz, M.-H., Vanhée, S., 2013. Potential impacts of extreme storm surges on a low-lying densely populated coastline: the case of Dunkirk area. Northern France. Natural Hazards 66 (3), 1327–1343. https://doi.org/10.1007/s11069-012-0210-9.
McNamara, D.E., Gopalakrishnan, S., Smith, M.D., Murray, A.B., 2015. Climate adaptation and policy-induced inflation of coastal property value. PLoS One 10 (3), e0121278. https://doi.org/10.1371/JOURNAL.PONE.0121278.
Mentaschi, L., Vousdoukas, M.I., Pekel, J.-F., Voukouvalas, E., Feyen, L., 2018. Global long-term observations of coastal erosion and accretion. Sci. Rep. 8 (1) https://doi.org/10.1038/s41598-018-30904-w. Article 1.
Merkens, J.L., Lincke, D., Hinkel, J., Brown, S., Vafeidis, A.T., 2018. Regionalisation of population growth projections in coastal exposure analysis. Clim. Chang. 151 (3–4), 413–426. https://doi.org/10.1007/S10584-018-2334-8/FIGURES/3.
Meur-Férec, C., Deboudt, P., & Morel, V. (2008). Coastal Risks in France: An Integrated Method for Evaluating Vulnerability. *Doi:*https://doi.org/10.2112/05-0609.1, *24* (sp2), 178–189. doi:https://doi.org/10.2112/05-0609.1.
Muis, S., Verlaan, M., Winsemius, H.C., Aerts, J.C.J.H., Ward, P.J., 2016. A global reanalysis of storm surges and extreme sea levels. Nature. Communications 7 (1). https://doi.org/10.1038/ncomms11969. Article 1.
Muis, S., Apecechea, M.I., Dullaart, J., de Lima Rego, J., Madsen, K.S., Su, J., Yan, K., Verlaan, M., 2020. A high-resolution global dataset of extreme sea levels, tides, and storm surges, including future projections. Front. Mar. Sci. 0, 263. https://doi.org/10.3389/FMARS.2020.00263.
Müller, B., Bohn, F., Dreßler, G., Groeneveld, J., Klassert, C., Martin, R., Schlüter, M., Schulze, J., Weise, H., Schwarz, N., 2013. Describing human decisions in agent-based models—ODD+D, an extension of the ODD protocol. Environ. Model. Softw. https://doi.org/10.1016/j.envsoft.2013.06.003.
Muriel, T., Abdelhak, N., Gildas, A., Francois, B., 2008. Assessing environmental benefits with the hedonic-price method: an application to coastal homes. Economie et Prevision 185 (4), 47–62. https://doi.org/10.3406/ECOP.2008.7837.
Neumann, B., Vafeidis, A.T., Zimmermann, J., Nicholls, R.J., 2015. Future coastal population growth and exposure to sea-level rise and coastal flooding—a global assessment. PLoS One. https://doi.org/10.1371/journal.pone.0118571.
Nicholls, R.J., 1998. Assessing erosion of sandy beaches due to sea-level rise. Geological Society, London, Engineering Geology Special Publications 15 (1), 71–76. https://doi.org/10.1144/GSL.ENG.1998.015.01.08.
Nicholls, R.J., Hinkel, J., Lincke, D., van der Pol, T., 2019. Global Investment Costs for Coastal Defense Through the 21st Century. https://doi.org/10.1596/1813-9450-8745.
Passeri, D.L., Hagen, S.C., Irish, J.L., 2014. Comparison of shoreline change rates along the South Atlantic bight and northern Gulf of Mexico coasts for better evaluation of future shoreline positions under sea level rise. J. Coast. Res. 68 (10068), 20–26. https://doi.org/10.2112/SI68-003.1.
Passeri, D.L., Hagen, S.C., Plant, N.G., Bilskie, M.V., Medeiros, S.C., Alizad, K., 2016. Tidal hydrodynamics under future sea level rise and coastal morphology in the Northern Gulf of Mexico. Earth's Future 4 (5), 159–176. https://doi.org/10.1002/2015EF000332.
Peterson, C.H., Bishop, M.J., 2005. Assessing the environmental impacts of beach nourishment. BioScience 55 (10), 887–896. https://doi.org/10.1641/0006-3568(2005)055[0887:ATEIOB]2.0.CO;2.
Pilkey, O.H., Young, R.S., Bush, D.M., 2000. Comment [on "Sea level rise shown to drive coastal erosion"]. EOS Trans. Am. Geophys. Union 81 (38), 436. https://doi.org/10.1029/00EO00327.
Poot, J., Alimi, O., Cameron, M.P., Maré, D.C., 2016. The gravity model of migration: the successful comeback of an ageing superstar in regional science. Investigaciones Regionales 2016 (36Specialissue), 63–86.
Poussin, J.K., Botzen, W.J.J.W., Aerts, J.C.J.H., 2013. Stimulating flood damage mitigation through insurance: an assessment of the french catnat system. Environmental Hazards 12 (3–4), 258–277. https://doi.org/10.1080/17477891.2013.832650.
Poussin, J.K., Botzen, W.J.W., Aerts, J.C.J.H., 2014. Factors of influence on flood damage mitigation behaviour by households. Environ. Sci. Pol. 40, 69–77. https://doi.org/10.1016/j.envsci.2014.01.013.
Poussin, J.K., Wouter Botzen, W.J., Aerts, J.C.J.H., 2015. Effectiveness of flood damage mitigation measures: empirical evidence from French flood disasters. Glob. Environ. Chang. 31, 74–84. https://doi.org/10.1016/j.gloenvcha.2014.12.007.
Pranzini, E., Wetzel, L., Williams, A.T., 2015. Aspects of coastal erosion and protection in Europe. J. Coast. Conserv. 19 (4), 445–459. https://doi.org/10.1007/s11852-015-0399-3.
Ramos, R. (2016). Gravity models: a tool for migration analysis. *IZA World of Labor*, *March*, 1–10. doi:10.15185/izawol.239.
Ranasinghe, R., 2020. On the need for a new generation of coastal change models for the 21st century. Scientific Reports 2020 10:1 10 (1), 1–6. https://doi.org/10.1038/s41598-020-58376-x.
Ravenstein, E.G., 1885. The Laws of migration. J. Stat. Soc. Lond. https://doi.org/10.2307/2979181.
Reimann, L., Jones, B., Bieker, N., Wolff, C., Aerts, J.C.J.H., Vafeidis, A.T., 2023. Exploring spatial feedbacks between adaptation policies and internal migration patterns due to sea-level rise. Nature. Communications 14 (1). https://doi.org/10.1038/s41467-023-38278-y. Article 1.
Robert, S., Schleyer-Lindenmann, A., 2021. How ready are we to cope with climate change? Extent of adaptation to sea level rise and coastal risks in local planning documents of southern France. Land Use Policy 104, 105354. https://doi.org/10.1016/j.landusepol.2021.105354.
Saengsupavanich, C., Pranzini, E., Ariffin, E.H., Yun, L.S., 2023. Jeopardizing the environment with beach nourishment. Sci. Total Environ. 868, 161485 https://doi.org/10.1016/j.scitotenv.2023.161485.
Schaffar, A., Dimou, M., Mouhoud, E.M., 2019. The determinants of elderly migration in France. Pap. Reg. Sci. 98 (2), 951–972. https://doi.org/10.1111/pirs.12374.
Schiavina, M., Freire, S., MacManus, K., 2019. GHS population grid multitemporal (1975, 1990, 2000, 2015) European Commission, Joint Research Centre (JRC). http://data.europa.eu/89h/0c6b9751-a71f-4062-830b-43c9f432370f.

Scussolini, P., Aerts, J.C.J.H., Jongman, B., Bouwer, L.M., Winsemius, H.C., de Moel, H., Ward, P.J., 2016. FLOPROS: an evolving global database of flood protection standards. Nat. Hazards Earth Syst. Sci. 16 (5), 1049–1061. https://doi.org/10.5194/nhess-16-1049-2016.

Simon, H.A., 1955. A behavioral model of rational choice. Q. J. Econ. https://doi.org/10.2307/1884852.

Sjaastad, L.A., 1962. The costs and returns of human migration. In Source. J. Polit. Econ. 5; Vol. 70, 80–93.

Speybroeck, J., Bonte, D., Courtens, W., Gheskiere, T., Grootaert, P., Maelfait, J.-P., Mathys, M., Provoost, S., Sabbe, K., Stienen, E.W.M., Lancker, V.V., Vincx, M., Degraer, S., 2006. Beach nourishment: an ecologically sound coastal defence alternative? A review. Aquat. Conserv. Mar. Freshwat. Ecosyst. 16 (4), 419–435. https://doi.org/10.1002/aqc.733.

Spodar, A., Héquette, A., Ruz, M.-H., Cartier, A., Grégoire, P., Sipka, V., Forain, N., 2018. Evolution of a beach nourishment project using dredged sand from navigation channel, Dunkirk, northern France. J. Coast. Conserv. 22 (3), 457–474. https://doi.org/10.1007/s11852-017-0514-8.

Stive, M.J.F., 2004. How important is global warming for coastal erosion? Clim. Chang. 64 (1), 27–39. https://doi.org/10.1023/B:CLIM.0000024785.91858.1d.

Temmerman, S., Meire, P., Bouma, T.J., Herman, P.M.J., Ysebaert, T., De Vriend, H.J., 2013. Ecosystem-based coastal defence in the face of global change. Nature 2013 504:7478 504 (7478), 79–83. https://doi.org/10.1038/nature12859.

Tierolf, L., Haer, T., Botzen, W.J.W., de Bruijn, J.A., Ton, M.J., Reimann, L., Aerts, J.C.J.H., 2023. A coupled agent-based model for France for simulating adaptation and migration decisions under future coastal flood risk. Sci. Rep. 13(1), Article 1 https://doi.org/10.1038/s41598-023-31351-y.

Tiggeloven, T., de Moel, H., Winsemius, H.C., Eilander, D., Erkens, G., Gebremedhin, E., Diaz Loaiza, A., Kuzma, S., Luo, T., Iceland, C., Bouwman, A., van Huijstee, J., Ligtvoet, W., Ward, P.J., 2020. Global-scale benefit–cost analysis of coastal flood adaptation to different flood risk drivers using structural measures. Nat. Hazards Earth Syst. Sci. 20 (4), 1025–1044. https://doi.org/10.5194/nhess-20-1025-2020.

Toimil, A., Álvarez-Cuesta, M., Losada, I.J., 2023. Neglecting the effect of long- and short-term erosion can lead to spurious coastal flood risk projections and maladaptation. Coast. Eng. 179, 104248 https://doi.org/10.1016/j.coastaleng.2022.104248.

Tourment, R., Beullac, B., Peeters, P., Pohl, R., Bottema, M., Van, M., Rushworth, A., 2018. European and US levees and flood Defences characteristics. Risks and Governance. 173.

van Vuuren, D.P., Edmonds, J., Kainuma, M., Riahi, K., Thomson, A., Hibbard, K., Hurtt, G.C., Kram, T., Krey, V., Lamarque, J.F., Masui, T., Meinshausen, M., Nakicenovic, N., Smith, S.J., Rose, S.K., 2011. The representative concentration pathways: an overview. Clim. Chang. 109 (1), 5–31. https://doi.org/10.1007/S10584-011-0148-Z/TABLES/4.

van Vuuren, D.P., Kriegler, E., O'Neill, B.C., Ebi, K.L., Riahi, K., Carter, T.R., Edmonds, J., Hallegatte, S., Kram, T., Mathur, R., Winkler, H., 2014. A new scenario framework for climate change research: scenario matrix architecture. Clim. Chang. 122 (3), 373–386. https://doi.org/10.1007/s10584-013-0906-1.

Vitousek, S., Barnard, P.L., Fletcher, C.H., Frazer, N., Erikson, L., Storlazzi, C.D., 2017. Doubling of coastal flooding frequency within decades due to sea-level rise. Sci. Rep. https://doi.org/10.1038/s41598-017-01362-7.

Vousdoukas, M.I., Mentaschi, L., Voukouvalas, E., Verlaan, M., Jevrejeva, S., Jackson, L. P., Feyen, L., 2018. Global probabilistic projections of extreme sea levels show intensification of coastal flood hazard. Nature. Communications 9 (1). https://doi.org/10.1038/s41467-018-04692-w. Article 1.

Vousdoukas, M.I., Ranasinghe, R., Mentaschi, L., Plomaritis, T.A., Athanasiou, P., Luijendijk, A., Feyen, L., 2020. Sandy coastlines under threat of erosion. In Nature Climate Change. https://doi.org/10.1038/s41558-020-0697-0.

Ward, P.J., Winsemius, H.C., Kuzma, S., Bierkens, M.F.P.P., Bouwman, A., Moel, H.D., Loaiza, A.D., Eilander, D., Englhardt, J., Gilles, E., Gebremedhin, E.T., Iceland, C., Kooi, H., Ligtvoet, W., Muis, S., Scussolini, P., Sutanudjaja, E.H., Beek, R.V., Bemmel, B.V., Luo, T., 2020. Aqueduct floods methodology. In *World Resources Institute* (January; pp. 1–28). https://www.wri.org/research/aqueduct-floods-methodology. www.wri.org/publication/aqueduct-floods-methodology.

Zhang, K., Douglas, B.C., Leatherman, S.P., 2004. Global warming and coastal erosion. Clim. Chang. 64 (1), 41. https://doi.org/10.1023/B:CLIM.0000024690.32682.48.